Tracking viral entry into target cells by virological and immunological methods

Martin Fitzpatrick

A thesis submitted to the University of Birmingham for the degree of

MRES BIOMEDICAL RESEARCH

Supervisors Dr Claire Shannon-Lowe, Dr Heather Long

Table of Contents

Table of Figures

Table of Abbreviations

BART BamH1-A rightward transcript

CD4 Cluster of differentiation 4; T cell receptor co-receptor found on T_h, T_{reg} cells

CD8 Cluster of differentiation 8; T cell receptor co-receptor found on CTLs

CD21 Cluster of differentiation 8; Complement receptor 2, present on the B cell surface

EBV Epstein-Barr virus

EEA1 Early Endosome Antigen 1; early endosome marker

EBNA EBV nuclear antigen

EBER EBV-encoded RNA

HLA Human leukocyte antigen; major histocompatibility complex (MHC) in humans

IFN-γ Interferon gamma; immune stimulation in infection, macrophage activation

Lamp1 Lysosomal-associated membrane protein 1; late endosome marker

PBMC Peripheral blood mononuclear cell; lymphocytes, monocyte, macrophage

LMP Latent membrane protein; EBV

Rab5 Ras-related protein Rab-5; early endosome marker

Abstract

Epstein-Barr virus is a γ-herpesvirus endemic (>90%) in the human population and implicated in a variety of lymphomas and solid tumours including Hodgkin's lymphoma, Burkitt's lymphoma and post-transplant lymphoproliferative disorder. Despite the prevalence of EBV, little is known about the mechanisms of early infection, including the role of the various membrane glycoproteins to entry, fusion and escape. Additionally, although the long term immune response is well characterised, the contribution of CD4+ and CD8+ T cell recognition to surveillance of primary cellular infection is not known. In order to further understand the processes of virus entry and processing we have used a panel of glycoprotein knockout viruses and viral epitope-specific CD4+ CD8+ T cell clones to study EBV infection of primary B cells. We have shown that following binding uptake is rapid yet selective, with suggested roles for gp42 and gp85 in attachment and initiation of fusion. Endocytosis results in rapid up-regulation of primary resting B cell endosomal activity, although no further surface-bound EBV is internalised. Endosomal trafficking of endocytosed virus is rapid, reaching the late endosomal compartment within the first hour, and subsequent HLA class II loading and presentation within 8 hours of binding. Further, both membrane and capsid proteins were seen in the late endosome by confocal, indicating relatively low fusion efficiency. The endocytic/HLA class II pathway may therefore offer a promising target for CD4+ T cell immunotherapy offering a first line of defence during *de novo* infection.

1 Introduction

1.1 EBV

Epstein-Barr virus is a γ-herpesvirus endemic (>90%) in the human population[1]. Primary infection with EBV normally occurs in childhood and is typically asymptomatic. However, if delayed until adolescence, primary exposure may present as the acute disease infectious mononucleosis (IM)[2]. First discovered in cultured cells derived from Burkitt's lymphoma a childhood tumour common to the malarial belt of sub-Saharan Africa, EBV has subsequently been associated with the development of a variety of lymphomas and solid tumours including Hodgkin's lymphoma (HL) and nasopharyngeal carcinoma[3]. Despite the endemic spread of EBV, and the demonstrated transformative capability of EBV on B cells *in vitro*, incidence of EBV-related malignancy in the general population remains low. The importance of continued immune surveillance in prevention of progression to malignancy is shown by the increased incidence of EBV-related malignancies, such as post-transplant lymphoproliferative disorder (PTLD) or HL, following immune suppression[3]. Structurally, EBV consists of a double stranded 172kb DNA genome encapsulated by a nucelocapsid. The virus is enveloped with a number of glycoprotein spikes with important roles in viral entry and immune recognition. In common with other members of the herpesvirus family, following infection the virus persists in a latent state with sporadic reactivation into the lytic replication cycle resulting in shedding of the virus. Two EBV subtypes EBV-1 & EBV-2 exist in the wild, differentiated by EBNA2 gene sequence, with EBV-2 less effective at transforming B cells in vitro[4].

1.2 Life cycle of EBV

While little is known of early lytic to latent infection *in* vivo, research has established a common sequence of gene expression patterns, or latency programmes, in infected B cells following infection *in vitro* (Table 1). Latency III expression is associated with expression of up to 9 EBV proteins including nuclear antigens EBNA1, 2, 3A, 3B, 3C and LP, and the latent membrane proteins LMP1, 2A and 2B[5]. Additionally, two EBV-encoded no translated RNA are seen during latency EBERs (EBV-encoded RNAs) and BARTs (BamH1-A rightward transcripts). Sequential down-regulation of these latency genes is central role in EBV evasion of the host immune response. At latency O expression of EBNAs and LMPs (except LMP2A) are fully suppressed.

	EBERs	EBNA1	LMP1	LMP2A	EBNA2	ENBA3s EBNA-LP	
O	+		-	+	-	-	Memory B cells
I	+	+	-	-	-	-	BL, PEL
II	+	+	+	+	-	-	HL
III	+	+	+	+	+	+	PTLD
IV			-		+		IM, PTLD

Table 1. EBV gene expression in latency programmes 0-IV. Adapted from Küppers, R. B cells under influence [5]

1.2.1 Primary Infection to Latency

In primary infection EBV enters the host via the oral route (Figure 1). Infection of local epithelial cells in the oropharynx results in lytic replication and a high titre shedding of virus in the host's saliva which may persist up to 6 months post-infection[6]. Infection of local tissue B lymphocytes results in a growth transformed latency III population, expanding rapidly and migrating to the tonsils and other lymphoid tissues. Following infection of the B cell the viral DNA circularises via recombination of N-terminal repeats. This gives rise to circular episomes in the nuclei of infected cells, with a variable number of terminal repeats, useful in studying the clonality of lymphomas[7]. The majority of EBV positive B cells produced during expansion are eliminated by the emerging cytotoxic T

cell response to lytic and latent antigens. However, a proportion of these cells will successfully evade immune targeting by the down-regulation of gene expression and adoption of a latency 0 expression programme. These infected cells, characterised by expression of EBERs and perhaps LMP2A, persist in the host as part of the memory B-cell reservoir.

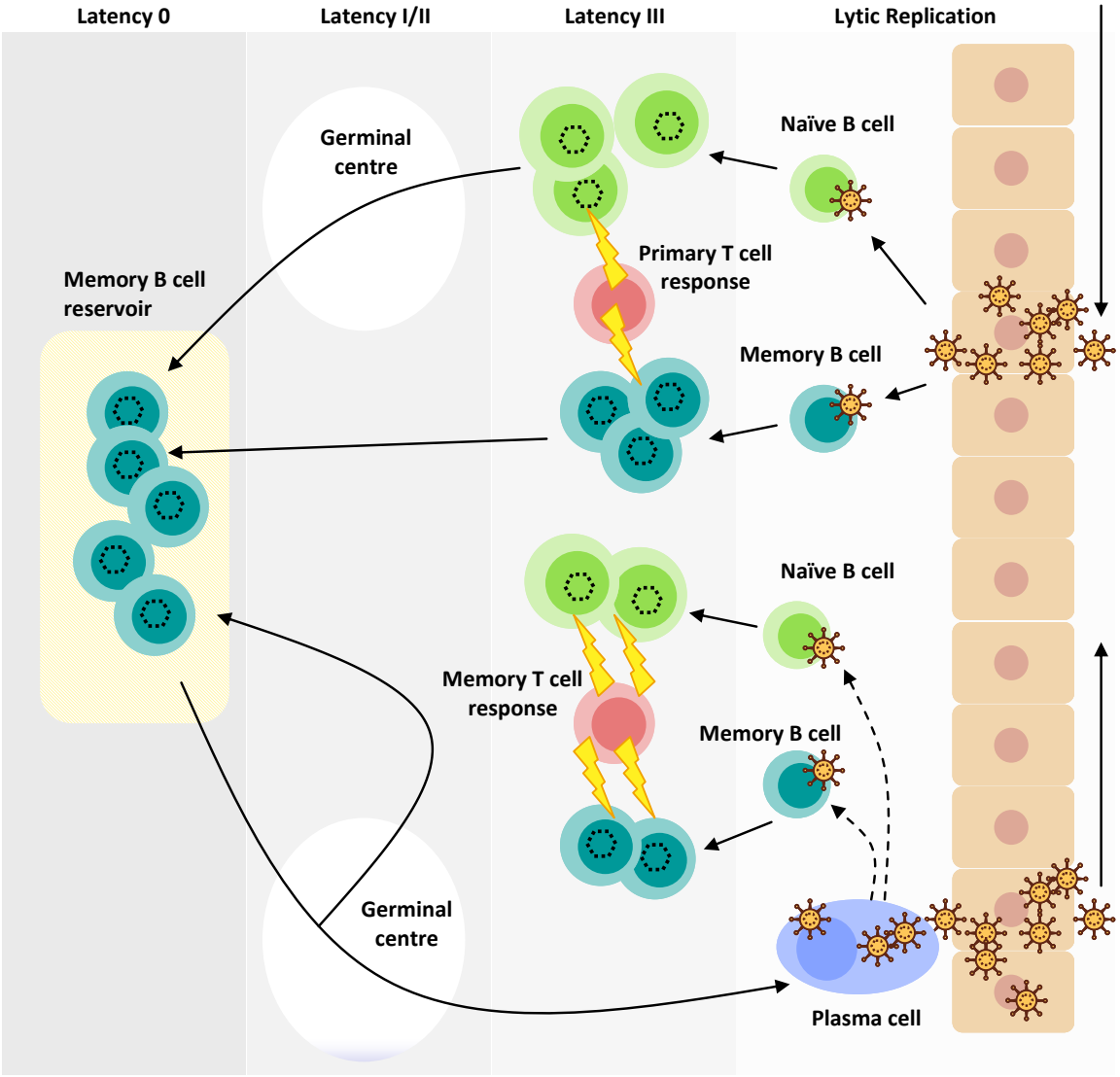

Figure 1. Life cycle of EBV. Adapted from Epstein Barr: 40 years on Lawrence S. Young and Alan B. Rickinson Nat. Rev. Cancer[8]

While EBV infects both naïve and memory B cells *in vitro* it is presently unknown whether *in vivo* EBV directly infects naïve B cells and viral transformation drives the

cells into a memory phenotype by mimicking antigen-specific somatic hyper-mutation in the germinal centre, or whether pre-existing populations of memory B cells are infected directly by EBV. Infected naïve B cells are occasionally observed in the germinal centre and do undergo clonal expansion in the absence normal selection. However, infection may occur in the germinal centre or alternatively the cells may be infected elsewhere and migrate there. However, during acute IM infected B cells are seen to preferentially migrate to the extra-follicular space in the tonsils, where expansion in the absence of somatic hyper-mutation results in Ig null mature B cells in circulation.

1.2.2 Latency to Lytic reactivation

Post infection carrier status is attained, with periodic low level shedding in the saliva of the infected host. The lifecycle of Epstein-Barr virus follows the pattern of latency in the B cell compartment, with cyclic lytic infection of epithelial cells and shedding from the oropharynx via the oral route. In rare cases EBV is also able to infect T cells, NK cells and smooth muscle cells and possibly monocytes[9], though the mechanisms involved are unclear and the role of these cells in the normal EBV life cycle is not known. The commitment of a large proportion of the host immune response to EBV lytic antigens suggests frequent reactivation and expression of lytic cycle proteins must occur *in vivo*.

1.2.3 Cellular and host responses to EBV infection

Acute infectious mononucleosis is associated with strong cellular immune responses, with expansion of oligoclonal EBV specific cytotoxic CD8+ T cells against both lytic and latent EBV antigens[10]. During this period responses to individual lytic epitopes can account for up to 40% of the CD8+ T cell population, with latent epitopes accounting for just 0.1-5%[11]. Studies of memory CD8+ responses have focused primarily on healthy individuals with no history of IM. These patients typically have lower virus titres in the throat and lower numbers of infected B cells in circulation. Appropriately, the majority of CD8+ memory cells show a resting phenotype and lack CD38/69 activation markers.

However, a proportion of EBV-specific CD8+ memory T cells do express perforin and are capable of targeted killing of peptide loaded cells *ex vivo*[12]. This EBV specific response is maintained in the host, with individual lytic and latent epitopes accounting for 0.2-2% and 0.05-1% of the CD8+ T cell population respectively[13]. In total EBV antigens account for approximately 5% of the CD8+ T cell pool, persisting and rising to up to 14% of CD8+ T cells by the age of 60 years[14]. Screening of IM patients has identified CD8+ responses to a wide range of lytic antigens including immediate early BZLF1 and BRLF1 and early proteins induced by these two including BMLF1, BMRF1, BALF1, BALF5[15]. Responses to other early or late antigens are seen in only a small number of patients and at low levels[10,16]. Latent antigens are also targeted for CD8+ response, predominantly from the EBNA3 family of proteins, but also LMP2 and EBNA1&2 to a lesser extent[17].

The role of the CD4+ response in EBV is less understood. Limited expansion of the CD4+ T cell pool is observed during IM in primary infection[18] although EBV-specific T cell responses are detectable at low levels, comparable to that seen in other viral infections[19]. Responses are to a broad range of lytic and latent antigens including immediate early protein BZLF1 and less frequently EBNA1[20]. In contrast to CD8+, considerable responses are also seen to late antigens[21]. Following the acute phase of IM CD4+ responses fall rapidly within the following weeks and have been difficult to study in detail. However, it has been shown that the majority of EBV-specific CD4+ T cells produce IFN-y and TNF-a, with a small proportion producing IL-2, and have a CD45RO+, CD27+, CD28+ phenotype[18]. Elispot assays show CD4+ memory T cell IFN-y responses to both latent EBNA and LMP derived antigens, with up to 60% of Caucasian donors recognising epitopes in EBNA1 and EBNA2[22]. However the majority of CD4+ responses are directed against lytic cycle antigens including BZLF1, BMLF1 and BHRF1, and to envelope glycoproteins gp350 and gp110 which are rarely targeted via the CD8+ response[23,24]. While CD4+ responses have been shown to be required to maintain an

effective CD8+ response, it is suggested that additionally some elements of the CD4+ response have direct cytotoxic action against latent antigen-positive cells[25]. While the importance of these CD4+ responses in vivo is unclear, the success of immunotherapy in lymphoproliferative disease is closely linked to the proportion of lytic antigen specific CD4+ T cells infused[26].

1.3 EBV mechanisms of infection

1.3.1 Attachment

During infection of B cells, the initial attachment occurs via high affinity interaction between gp350/220 and CR2 (CD21) (Figure 2, Table 2). Binding triggers capping of CR2 on the B cell surface and subsequent endocytosis of the viral particle into a low pH early endosomal compartment[27]. Antibodies to gp350 and soluble CR2 both inhibit infection of B cells via this CR2 dependent mechanism[28]. Recombinant viruses lacking gp350 may still transform B cells but do so with much reduced efficiency, suggesting that while not necessarily the only route for B cell entry, it is by far the dominant one[29].

Infection of epithelial cells is more complex, with multiple apparently redundant routes of attachment. Some epithelial cells do express CR2/CD21at low levels in culture and so can be bound by gp350[30]. However, it is unclear what contribution this makes *in vivo* as in contrast to B cells antibodies to gp350 *enhance* infection of epithelial cells with the binding of anti-gp350 immunoglobulin-A coated virus to the polymeric IgA receptor, having a possible role in basolateral infection or *trans*-migration in epithelia[31]. Epithelial cell infection with cell-free virus shows very poor efficiency[32] *in vitro* however the recently discovered mechanism of 'transfer infection' from adjacent B cells results in much improved uptake[33]. This has particularly important implications for virus shedding during reactivation. IgA antibody release at mucus membranes is dependent on close association of plasma B cells and the basolateral epithelium with release of IgA

occurring *through* the epithelial cell via endocytosis[34]. The close association of potentially infected B cells, the much increased infection efficiency via transfer, and the putative role of gp350 IgA in epithelial attachment strongly suggests that this mechanism may be the predominant route for epithelial cell infection *in vivo*. Absence of CR2 the gHgL (gp85/gp25) complex has additionally been shown to facilitate entry to epithelial cells[35] via an as yet unknown receptor, and antibody to this complex inhibits uptake[36]. Additionally, a protein encoded by the BMRF2 open reading frame has been shown to interact with β1, α5, α3 and αv integrins and may bind epithelial cells[32,37], although only small quantities of BMRF2 are found in the virus particle[38].

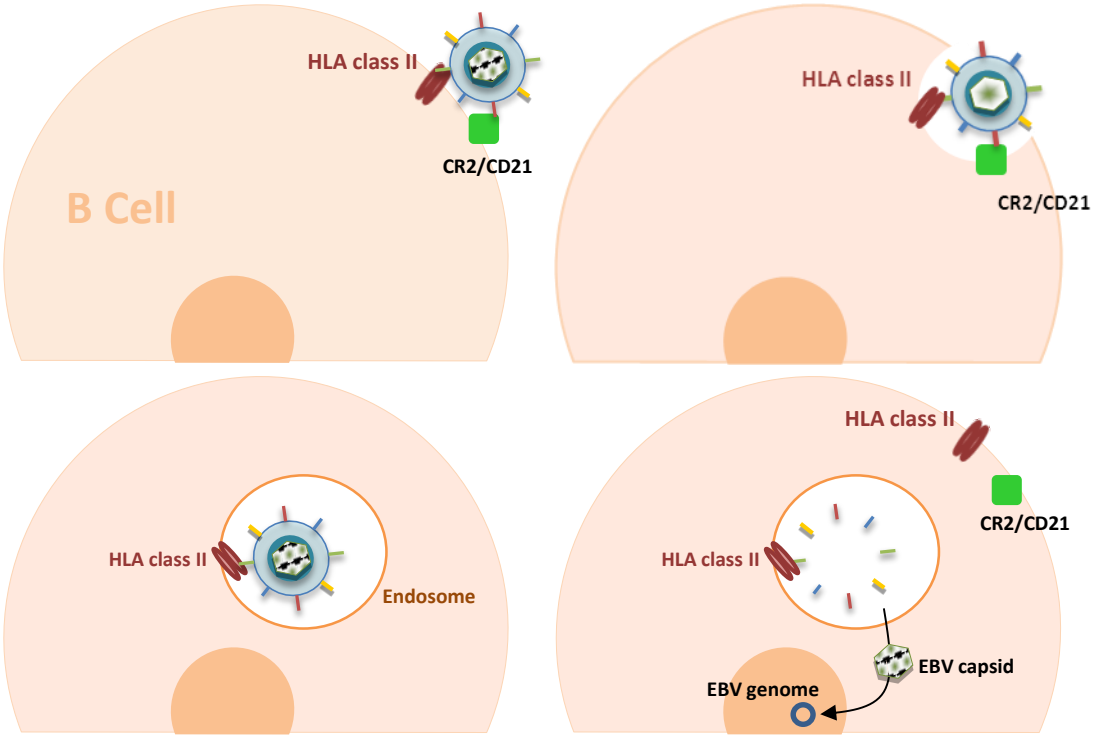

Figure 2. Schematic of EBV cellular entry and fusion processes in B cells. Binding of gp350 to CD21/CR2 of the surface, triggers internalisation to the endocytic pathway. Interaction of gp42 with HLA class II triggers fusion and release of the viral genome to the cytosol.

1.3.2 Fusion & penetration

Fusion and internalisation of EBV is dependent on the presence of three glycoproteins common to all herpesvirus family members: gH, gL and gB (gp85, gp25, gp110)[39]. However, the role and importance of these glycoproteins differs between target cells.

Fusion of EBV with B cells is endocytosis dependent, triggered by the interaction between gp350/220 and CR2 on the cell surface[40]. Fusion occurs in a low pH compartment and requires gHgL, gB (gp85) in addition to gp42, a type-II membrane protein which associates noncovalently with the gHgL complex. Interaction between this gHgLgp42 complex and HLA class II in the endosomal pathway is thought to trigger fusion of the viral envelope and penetration of the capsid into the cytosol[41]. Binding of the gp42 to HLA class II is allele specific, with the virus unable to bind to rare HLA-DQs, however due the existence of multiple HLA types within an individual it is unlikely to have substantial importance *in vivo*[42]. Interactions occur with both immature and peptide loaded MHC indicating that binding occurs not at the peptide groove itself.

Fusion of EBV with epithelial cells is endocytosis independent and occurs at neutral pH. There is no constitutive expression of HLA class II on epithelial cells, and the presence of gp42 in the infecting virion is unnecessary and in fact *inhibitory* for infection[43]. Wild type EBV has lower expression of gp42 than gHgL suggesting that gHgL can operate independently to enable epithelial entry by another as yet unknown target. Epithelial fusion is also dependent on higher levels of gB than that seen in B cells[44], although the mechanics of gB in epithelial fusion remain unclear.

As the gHgL and gHgLgp42 complexes differentially aid entry into epithelial and B cells respectively, the relative quantity of each complex on the virion surface has been suggested as a determinant of viral tropism. Viruses produced in epithelial cells are

gHgLgp42 rich, while in B cells the interaction of gp42 with immature HLA class II and subsequent degradation results in virions that are gHgLgp42 low, and gHgL high. As a result, virus produced in B cells is more able to infect epithelial cells, and likewise, virus produced in epithelial cells is more able to infect B cells[45]. Binding of EBV to B cell surface has subsequently been shown to significantly enhance secondary infection of epithelial cells, without internalisation or active infection of the B cell occurring[33].

Gene	Protein	Pass/Type	Role in EBV entry
BLLF1	gp350	Single/1	Attachment B-cell receptor CR2/CD21
BXLF2	gp85/gH	Single/1	Fusion; Attachment epithelial cell co-receptor
BKRF2	gp25/gL	Single/2	gH chaperone
BZLF2	gp42	Single/2	Fusion interacts with B-cell MHC-II
BALF4	gp110/gB	Single/1	Fusion
BLRF1	gN	Single/1	gM co-dependent, possible post-fusion
BBRF3	gM	Multispan	
BMRF2		Multispan	Attachment via integrins polarised epithelial infection

Table 2. Envelope glycoproteins of EBV involved in B and epithelial cell infection. Lindsey M. Hutt-Fletcher. Epstein-Barr Virus Entry (Minireview) JV 2007[46]

1.4 Host processing and presentation of antigens

Effective adaptive immune responses are dependent on the presentation of peptides derived from foreign antigens to the host T cells. Two distinct cellular pathways exist, broadly processing endogenous expressed or exogenously acquired antigen, culminating in the presentation of antigen on the cell surface via HLA class I and II respectively.

Peptides presented in the endogenous class I pathway are generated from the degradation of cytosolic proteins by the proteasome – including both host cell proteins and those of infecting agents. Proteosomal degradation is constitutive in all cells, but may be up-regulated in infected cells. Degraded proteins are trans-located into the endoplasmic reticulum via the transporter associated with antigen processing (TAP). Assembly of HLA class I molecules occurs in the endoplasmic reticulum with a complex including TAP, calnexin, Erp57, tapasin and calreticulin stabilising the structure until the

binding of peptide occurs. Once loaded the assembly complex dissociates and the HLA-I-peptide complex is transported through the secretory pathway to the cell surface undergoing various post-translational modifications in the Golgi apparatus. Once on the cell surface HLA-I bound peptide epitopes are presented to CD8+ T cells for recognition.

In contrast peptides presented via the exogenous class II pathway are derived from extracellular proteins endocytosed and digested by the host cell. Not all cells express class II and process antigen in this way, but it is constitutively expressed in professional antigen cells including B cells, macrophages and dendritic cells, and inducible in other cells, such as activated epithelial cells, by the presence of IFNγ. As with class I, HLA class II molecules are assembled in the endoplasmic reticulum, however as binding of target peptide must occur in the late endosome, an invariant chain li, is bound in its place. The assembled HLA class II molecule is exported via the Golgi apparatus, and directed by li target sequence, fuses with the late endosome. Degradation of the invariant chain by cathepsins leaves a small CLIP fragment blocking the peptide binding groove. CLIP is in turn removed by class II like HLA-DM to enable peptide binding. The assembled peptide-HLA-II complex is then transported to the cell surface for CD4+ T cell recognition.

1.5 Research goals and study methods

Despite the relative prevalence of EBV in the population, relatively little is known about the infective process. For example, while a number of envelope glycoproteins are known to be essential for entry and infection, other glycoproteins have undefined roles and it remains unclear whether they act during fusion, migration and processing of the virus. Additionally, while immune recognition of actively infected cells is well studied, little is known of early recognition of infected B cells by CD4+ or CD8+ T cells, or which epitopes are targeted by the immune system. In order to study the timeline of infection we will use confocal microscopy, with fluorescently labelled antibodies to envelope

glycoproteins, allowing us to track progress through the cell. Further, IFNγ assay of T cell recognition of virion-borne epitopes will be used to determine uptake, processing and presentation by infected primary B cells. Lastly, selective knockout of viral glycoproteins will be used to try and ascertain the role of these in the infection process.

2 Materials & Methods

2.1 Media and Buffer Solutions

Cells	Hygromycin	Type	Vessel	Adherence
2089	20µl/10ml RPMI	Epithelial	10cm dish	Semi
BZLF1 KO	20µl/10ml RPMI	Epithelial	10cm dish	Semi
gp350 KO	20µl/10ml RPMI	Epithelial	10cm dish	Semi
gp42 KO	20µl/10ml RPMI	Epithelial	10cm dish	Semi
gp85 KO	20µl/10ml RPMI	Epithelial	10cm dish	Semi

Table 3. Cell culture lines used, all 2089 derived.

Coating buffer (10x stock)	Sodium carbonate	1.36g
	Potassium bicarbonate	7.35g
	- Make up to 100ml H20	
	- Adjust to pH9.2 1M HCl/1M NaOH	
Blocking buffer	PBS	500mls
	Bovine serum albumin	5g
	Tween	250µl
Wash buffer	PBS	5L
	Tween	2.5ml

Table 4. Solutions for IFNγ ELISA

2.2 Antibodies

Species	Target	Dilution	Identifies
Mouse	gp42	1/500	Glycoprotein gp42
Mouse	gp110	1/500	Glycoprotein gp110
Mouse	gp350	1/500	Glycoprotein gp350
Rat	p18	1/500	Capsid protein
Rabbit	LAMP1	1/500	Late endosomes/lysosomes
Rabbit	Rab5	1/500	Early endosomes
	IFNγ		IFNγ

Table 5. Primary antibodies for immunofluorescence and ELISA

Species	Target	Dilution	Conjugation	
Goat	anti-Rabbit	1/1000	Alexa fluor 594	Invitrogen
Goat	anti-Mouse	1/1000	Alexa fluor 488	Invitrogen
Goat	anti-Rat	1/1000	Alexa fluor 488	Invitrogen
	IFNγ		Streptavidin	

Table 6. Secondary antibody conjugates for immunofluorescence and ELISA

2.3 PBMC separation from whole blood

Blood was obtained from donations from healthy donors or from apheresis cones obtained from the NHSBT, Birmingham. Blood was diluted in an equal volume of PBS and layered on top of lymphoprep. Samples were centrifuged at 1800rpm for 30 minutes at room temperature. The separated PBMC layer was removed, washed twice in 50ml PBS at 1600 and 1200rpm and re-suspended in 10ml RPMI, 1% FCS. The total PBMC count was made and B cell numbers determined by assuming B cells account for 5% of total PBMC.

2.4 Isolation of B cells from PBMCs

Primary resting B cells were isolated from total PBMC by magnetic bead separation using CD19 Dynabeads, according to manufacturer's instructions. Briefly, B cells were incubated with 4 dynabeads at 4°C for 30 minutes, washed x 5 in RPMI, 1% FCS to ensure B cell purity, then the beads were removed by incubation with CD19 detachabeads for 45 minutes at room temperature.

2.5 Passage of virus-producing cell lines

The virus-producing 293 cell lines were maintained on 10cm plates in RPMI, 10% FCS, 1% glutamine, 1% Penicillin/streptomycin (full medium) and 50uM Hygromycin. Cells were passaged twice a week when approx. 80% confluent. Briefly, the cells were washed in PBS then were detached from the culture plates by incubation with 1ml trypsin at room temperature for 2 minutes. The trypsin was neutralized with RPMI, 10% FCS and a single cell suspension was passaged at 1 in 3 to fresh plates.

2.6 Induction of lytic replication in virus producing 293 cells

The 293 cells were grown to approx. 80% confluence on 10cm plates. The cells were removed from the plates by trypsinisation as above, then re-suspended in 28ml of fresh

full medium without hygromycin. This single cell suspension was plated onto 9 wells of two 6 well plates at 3ml per well and incubated at 37°C overnight. The following day, for each well of the 6 well plate, transfection mix was prepared: 100ul of OptiMEM was incubated with 6ul lipofectamine, 0.5ug BZLF1 (p509) and 0.5ug gp110 (pRA) expression plasmids for 20 minutes at room temperature. Following this incubation, the transfection mix was made up to 1ml with OptiMEM. All medium was removed from the 293 cells and replaced with 1ml transfection mix, incubated at 37°C for 3 hours then 1ml of full medium added without hygromycin. The virus was harvested after 3 to 5 days of incubation at 37°C, when the virus supernatant was removed, centrifuged to remove cells and filtered with a 0.45um syringe filter. The virus was frozen at -80°C until use.

2.7 Virus purification

Intact, enveloped virus particles were purified by density ultra-centrifugation on an Optiprep gradient. Sixty per cent Optiprep was diluted to 30% in Optiprep diluent (0.85% w/v NaCl, 60mM Hepes-NaOH, pH 7.4) and 1ml was added to a 14ml Beckman centrifuge tube. Eleven ml of virus supernatant was layered on the Optiprep and tube pairs balanced for ultracentrifugation in an SW40 (swing) rotor at 20,000rpm for 2 hours with max acceleration, slow deceleration to concentrate the virus on the Optiprep cushion. Following centrifugation, 10ml supernatant was removed and discarded, then the remaining 1ml concentrated virus and 1ml Optiprep cushion were mixed thoroughly to give a 15% solution of Optiprep. This was transferred to a 4.8ml Beckman ultracentrifuge tube, topped up with 15% Optiprep, balanced and the top sealed. The tubes were centrifuged in a vTi60.5 vertical rotor at 64,000rpm for 2 hours and 40 mins, 4°C with max acceleration and slow deceleration. Following centrifugation, the purified concentrated virus band, visible as a white layer towards the bottom of the tube, was removed by needle aspiration in a 200ul volume.

2.8 Virus titre quantification

Virus titre was quantified using quantitative PCR for the single copy EBV viral DNA polymerase gene. The concentrated virus was initially diluted 1 in 20 in DEPC water, then 10ul of diluted supernatant was incubated with 10ul of virus lysis buffer (1 x PCR buffer, 1% Triton-x-100, 0.1mg/ml proteinase K) at 55°C for 1 hour, followed by 95°C for 5 minutes to inactivate the proteinase K in the lysis solution. Five microliters of lysed virus was added to each PCR, with 1 x Taqman Universal PCR mastermix (Applied Biosystems), 12.5uM EBV DNA polymerase primers, 5pMol probe. Namalwa DNA (2 EBV genomes per cell) was used as the internal standard.

2.9 EBV infection and Cytospins

Aliquots of 1 x 10^6 primary resting B cells were initially incubated on ice with purified EBV at an MOI of 100, or uninfected, for 1 hour. Unbound virus was washed off and the cells re-suspended in 1ml total medium then incubated at 37°C for 30, 60, 90 and 120 minutes. Following each time point, the cells were washed in PBC and fixed in 1ml of 2% paraformaldehyde for 20 minutes at RT and 1 x 10^5 cells were subjected to cytospin onto poly-L-lysine-coated slides for 5 minutes at 1000rpm.

2.10 Immunofluorescence

Primary B cells and B cell lymphoblastoid cell lines were labelled with individual monoclonal antibodies (mAbs) or mAb combinations to minor capsid protein P18, gp350, early endosomes EA1 and late endosomes LAMP1. Antibodies were appropriately diluted (Table 5) in heat inactivated normal goat serum (HInGS). The cell spots generated by cytospin were isolated using a hydrophobic PAP pen. Slides were initially incubated in 0.1% glycine to reduce background staining caused by PFA fixation, then washed in PBS. The cells were permeabilised by incubation with 0.5% Triton-x-100 at RT for 5 minutes, washed in PBS then incubated with antibodies for 1 hour at 37°C in

a humidified chamber. The cells were washed three times for 5 minutes in PBS in a wash bath and incubated with appropriately-diluted secondary antibodies (Table 6) at 37°C for 30 minutes. Finally, the slides were washed x 5 in PBS as above, then mounted in Vectashield + DAPI to counterstain the nucleus.

2.11 Confocal microscopy

Stained B cells were viewed by confocal microscopy (Leica). Areas of apparent co-localisation were assessed by the confocal software and z-stack images taken of whole cells. Selected images were analysed to ImageJ software to assess co-localisation.

2.12 T cell assay

Primary B cells were isolated from lab donors and HLA matched to T cell clones targeting desired epitopes. Purified virus supernatant was added to target cells with 500ul RPMI+10% FCS to allow for gas exchange in presence of OptiPrep and left to bind on ice. After 1 hour samples were removed from ice and spun down at 5000rpm 4 mins to remove virus and re-suspended in fresh media. Cells were then incubated at 37'c for required time-course. Optionally fixation was performed by re-suspending cells in PBS then fixing with 1% PFA 1ml for 10 minutes before quenching with 9ml 0.2M glycine. Cells were washed twice and re-suspended in RPMI+10% FCS.

For each experiment protein standards were produced using known target peptides. Positive control was by lytic B95.8, with BZLF K/O LCL and primary B cells to confirm processing. Cells were re-suspended in 500ul RPMI+10% FCS and 1ul of each target peptide was added and incubated for 1 hour at 37'C. Pulses cells were then washed three times in RPMI+10% FCS then re-suspended at 100ul/target well.

Prepared cells were seeded to V-bottom plate at 5x104 B cells/well and 100ul/well. HLA matched T cell targets were seeded at 5000 T cells/well and left to incubate for required time. Resulting supernatants were harvested for IFNγ ELISA.

2.13 IFNγ ELISA

Maxisorp (Nunc) plates were coated with anti-human IFNγ stock antibody diluted in coating buffer with 50µl per well at a concentration of 0.75ug IFNγ/ml. Plates were left to block overnight at 4'c. The following day, antibody was flicked off and the plate blocked with blocking buffer at 200µl per well. A standard curve was prepared using stock IFNγ (1x10-3mg/ml) diluted at 4ul/2ml, giving 2000pg/ml, serially diluted to 31.25pg/ml final. An additional blank (no IFNγ) was prepared. Plate was washed with washing buffer 6 times, and then standards and test supernatants added, as per plate plan, at 50µl/well. A second plate, at 1/10 dilution was prepared using 45µl wash buffer, with 5µl supernatant. Plate was incubated for 2 hours at room temperature, then flicked off into Virkon and washed a further 6 times in wash buffer. Secondary biotinylated anti-IFNγ antibody was diluted in blocking buffer to 1/1333 dilution and added at 50µl/well to the plate. Plate was incubated at room temperature for 1 hour and then washed 6 times in wash buffer.

Extravidin peroxidise was diluted with blocking buffer 1/1000 and added at 50µl/well. Plate was incubated at room temperature for 30 minutes and then washed 10 times in wash buffer. 100µl of TMB substrate was added per well, left for 20 minutes to develop, and stopped with 1M HCl 100µl/well. Plate was read by spectrophotometer with absorbance 450nm and blank 655nm

3 Results

3.1 Primary resting B cells are endocytically inactive

It was first essential to determine the suitability of selected endosomal antibodies to visualise the endosomal pathway. Rab5 and EEA1 were selected as early endosomal markers, and Lamp1 as a late endosomal marker, and suitable antibodies to each of these were each titrated for confocal microscopy. Initial staining was performed on LCL cell lines which are known to be constitutively active, with uninfected primary B cells as a negative control for endosomes. The absence of endocytic activity in resting primary B cells, and relative abundance in constitutive LCLs was confirmed (Figure 3).

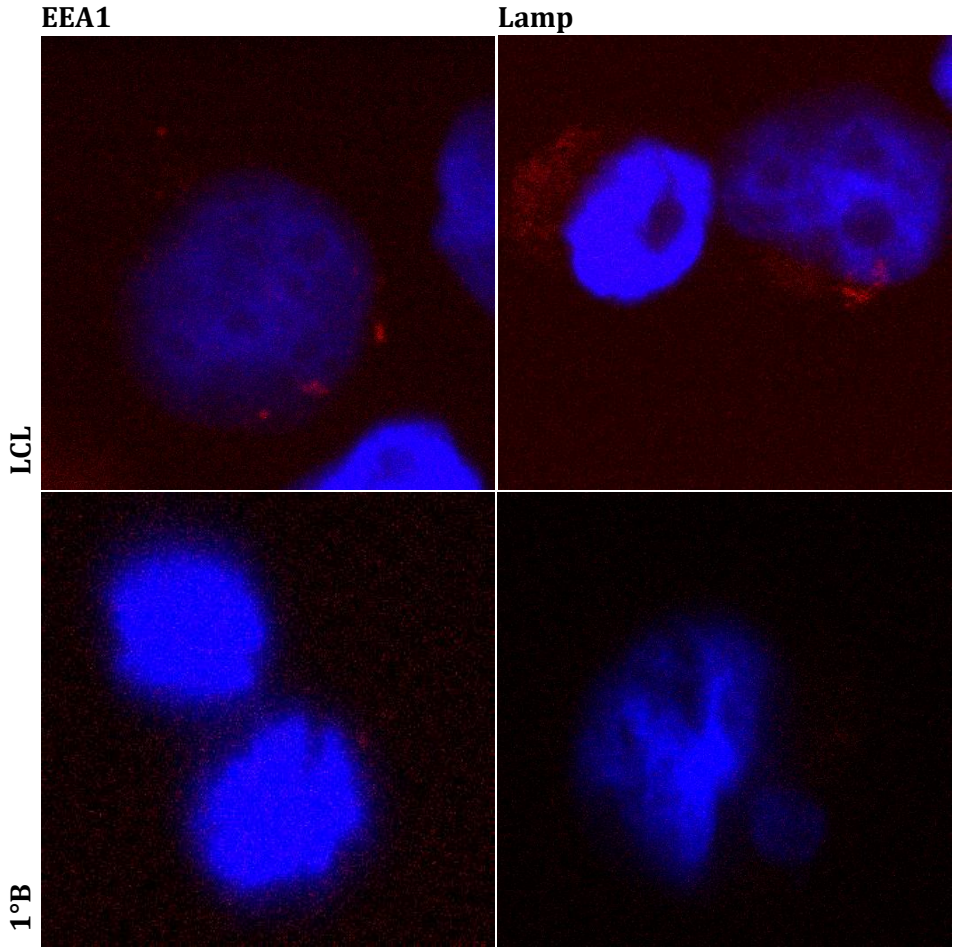

Figure 3. LCL and primary B cells with antibody staining for early (EEA1) and late (Lamp1) endocytic activity. Note the absence of endosomes in the primary B cells.

3.2 EBV infection up-regulates endocytosis in B cells

With these confirmed early and late endosomal markers, it was now possible to study the process of viral entry via the endosomal pathway. As before, a number of viral proteins were assayed for effectiveness using LCLs, with abundant glycoprotein gp350 and minor capsid antigen p18 providing consistent staining and subsequently used. Here, results showed a rapid increase in endocytic activity in primary B cells following binding and uptake of EBV visible at the 15 minute time-point (Figure 4).

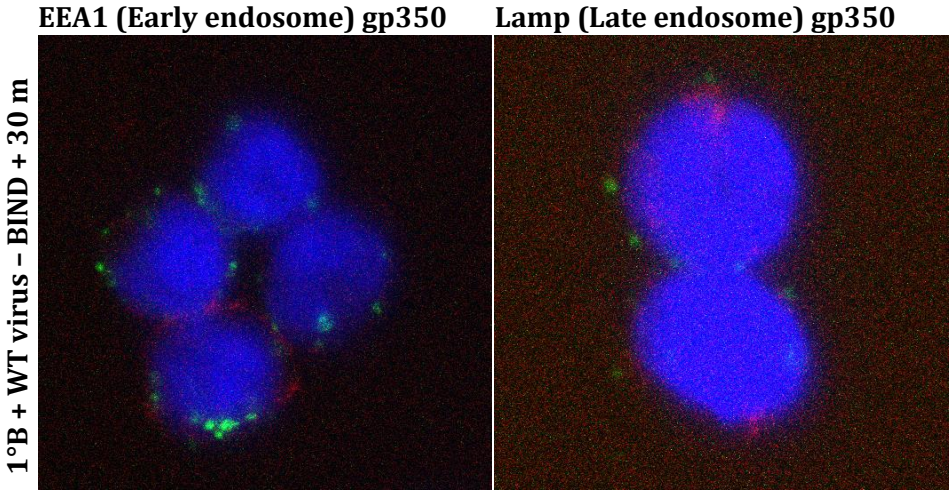

Figure 4. Early and late endosomal staining in primary B cells 15 minutes post-binding with EBV. Note the increased endocytic activity following uptake of the virus.

3.3 EBV proteins co-localise with early and late endosomes

To study the progression of endocytosed virus co-localisation of EBV proteins with early and late endosomal markers was analysed by confocal microscopy at serial time-points from 0 to 2 hours. Co-localisation of viral proteins with cellular early endosomal markers was observed at 15 minutes – the first time-point post-binding (Figure 5 & Figure 6). Co-localisation with early endosomal markers continued to be observed out to the 30 minute time-point after which it declines rapidly. At the final 120 minute time-point little to no co-localisation of viral proteins with early endosomal markers was

observed. In contrast, co-localisation of viral proteins with late endosomal markers was first observed from the 60 minute time-point (Figure 8 & Figure 8), with the exception of single image appearing to show small levels of co-localisation in a cell at 15 minutes. From 60 minutes onwards co-localisation continued with late endosomal marker Lamp1 out to the final 120minute time-point. Interestingly, we also observed that although the surface of primary B cells were frequently bound by multiple virions, relatively few virus particles were actually endocytosed – persisting until the 2 hour time-point with no apparent further uptake.

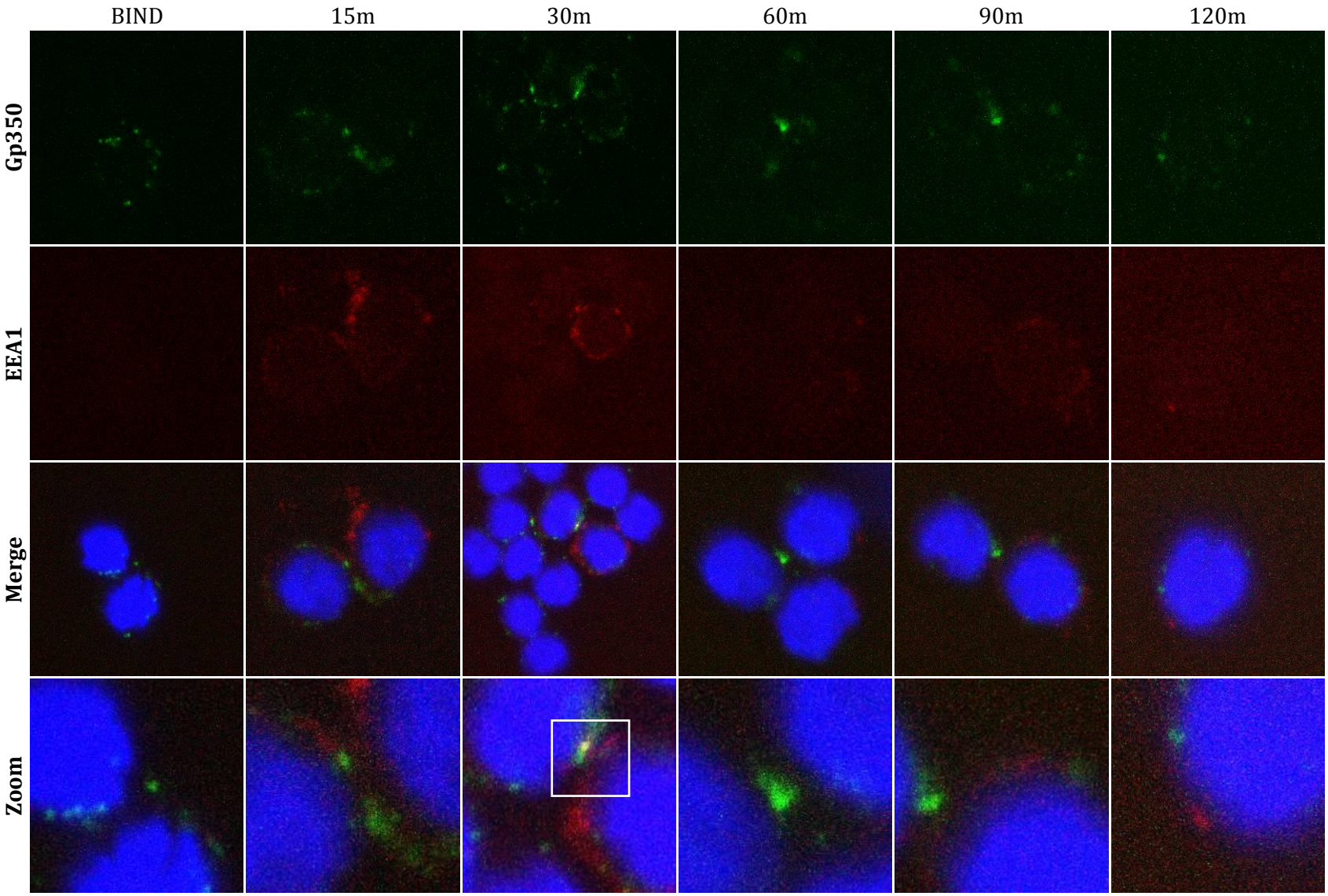

Figure 5. Early Endosomal Localisation (gp350/EEA1). Beginning of co-localisation of viral proteins and early endosomes is observed frequently from the earliest time-point at 15 minutes and reaching a peak at just 30 minutes post-binding.

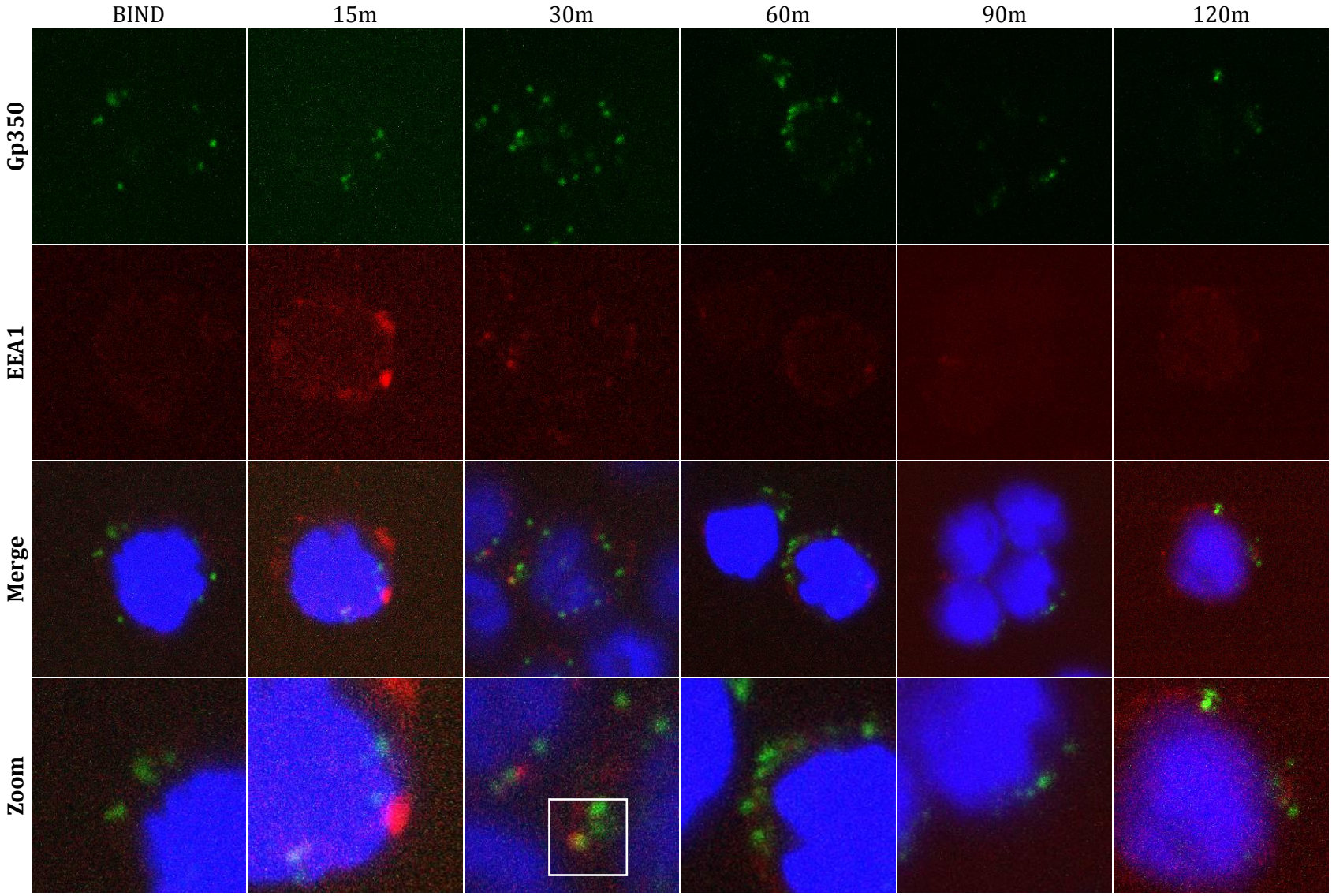

Figure 6. Early Endosomal Localisation (p18/EEA1). Beginning of co-localisation of viral proteins and early endosomes is observed frequently from the earliest time-point at 15 minutes and reaching a peak at just 30 minutes post-binding.

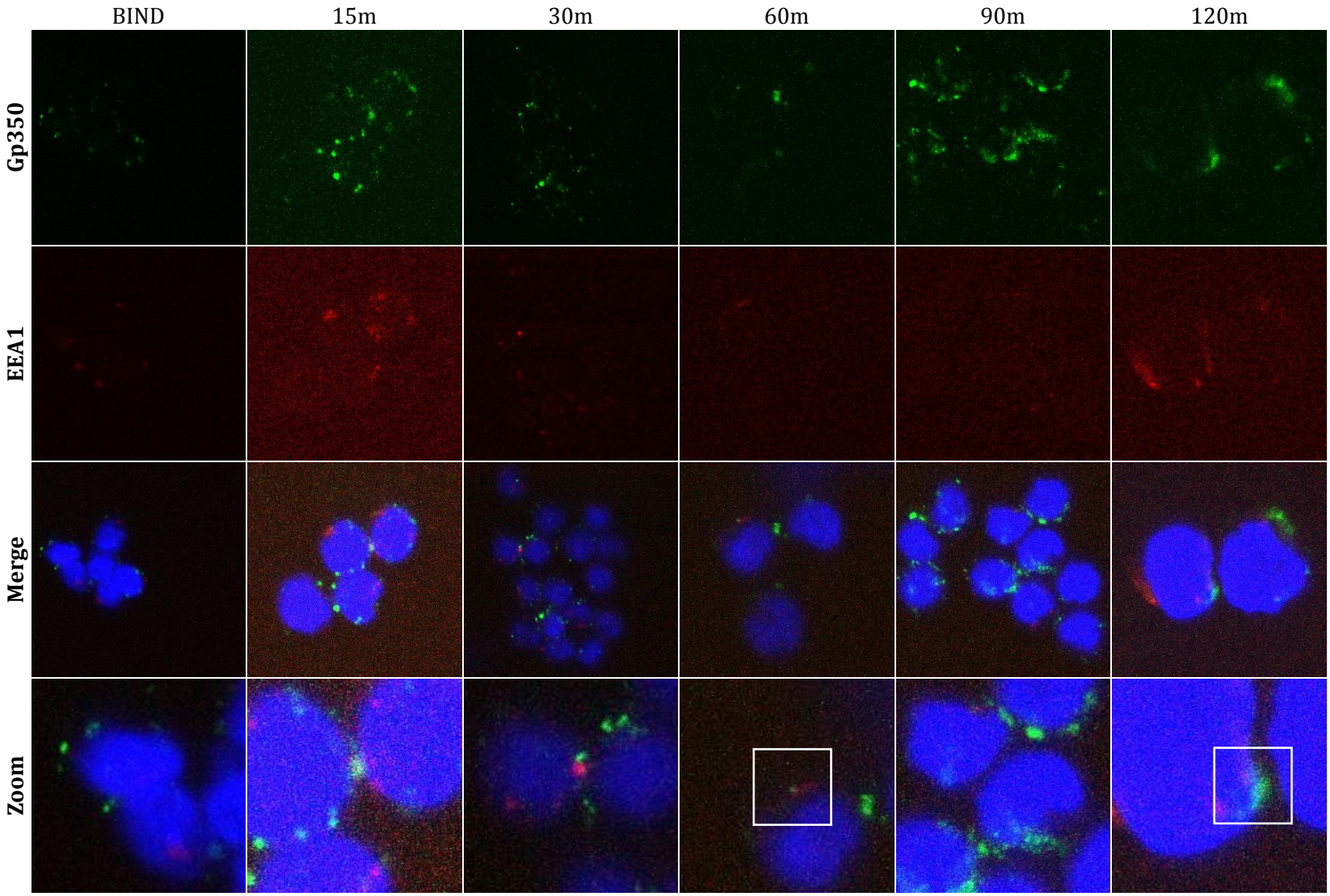

Figure 7. Late Endosomal Localisation (gp350/Lamp1). Co-localisation of viral proteins and late endosomal compartments peaks at the 60 minute time-point from binding, although in rare cases co-localisation with late endosomes is seen as early as 15 minutes.

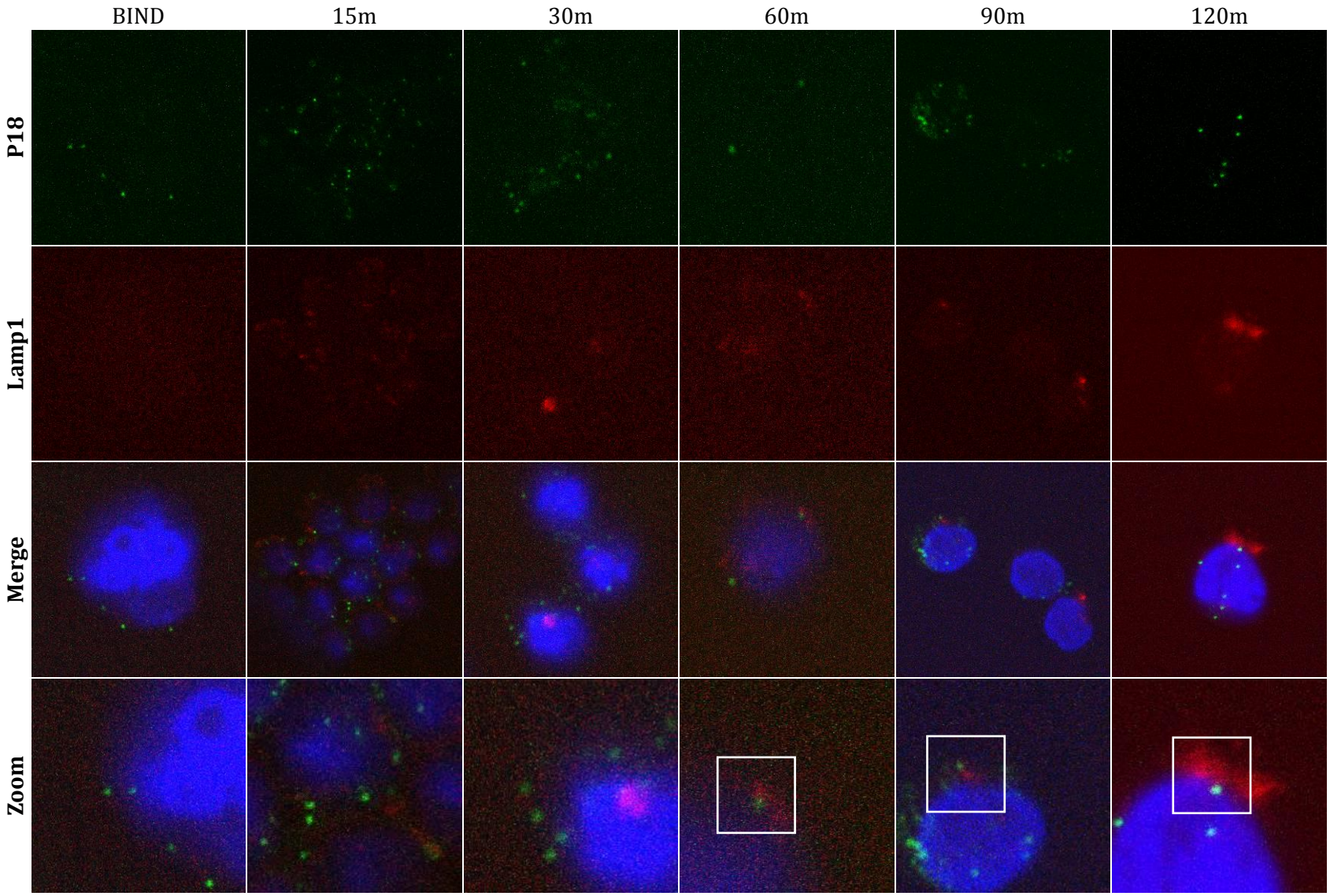

Figure 8. Late Endosomal Localisation (p18/Lamp1). Co-localisation of viral proteins and late endosomal compartments peaks at the 60 minute time-point from binding, although in rare cases co-localisation with late endosomes is seen as early as 15 minutes.

3.4 Functional avidity of EBV-specific CD4+ T cell clones

In order to study CD4+ T cell recognition of EBV-infected cells in the early hours post-infection a panel of available CD4+ T cells specific for various EBV antigens was used. Production of IFNγ observed during T cell recognition of cognate antigen is determined by both the quantity of peptide presented via HLA class II and the avidity of the T cell clone for the target epitope. As levels of presented peptide increase the likelihood of T cell recognition is increased, however in order to compare results between clones of different specificities the relative avidities were assessed. Thus, in future experiments variations in T cell response may be accurately accredited to variations in T cell avidity.

A panel of T cell clones selected for these experiments were assayed with known HLA-matched 1'B cells and known peptide concentrations from $1x10^{-11}$mg/ml to 1x10-5 mg/ml. Response curves were plotted and graphed (Figure 9) and EC50 were read coinciding with the straight logarithmic region of the curve. These EC50 values were used to compare each clone (Figure 10) demonstrating relatively similar functional avidities of T cell clones within groupings as follows: LDL & LEK, FLD & DNEc70 & VKF & PAQ and DNEc28 & VKL.

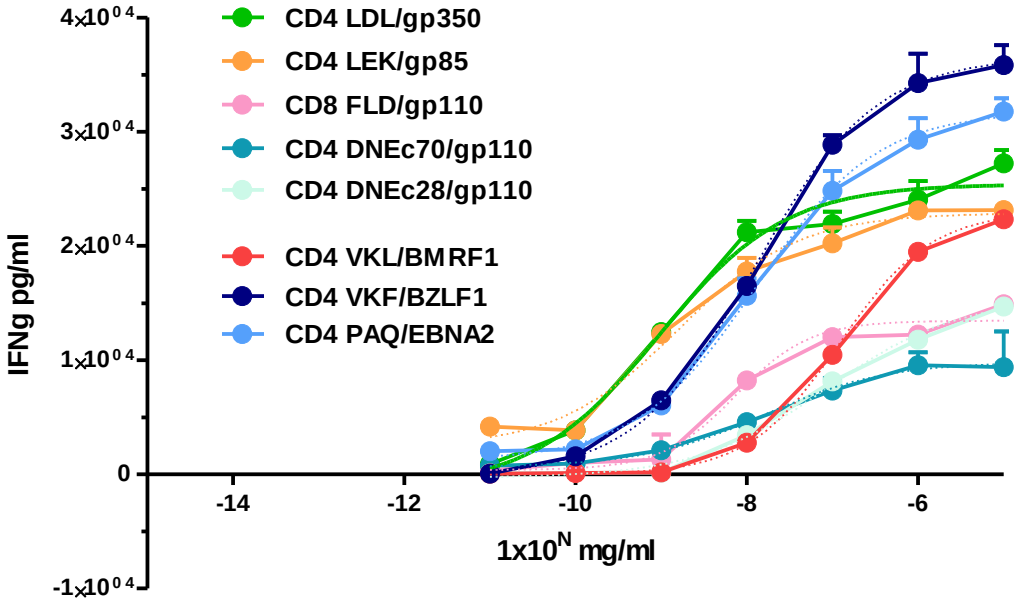

Figure 9. Relative IFNγ responses by T cell clones, matched concentrations of target epitopes.

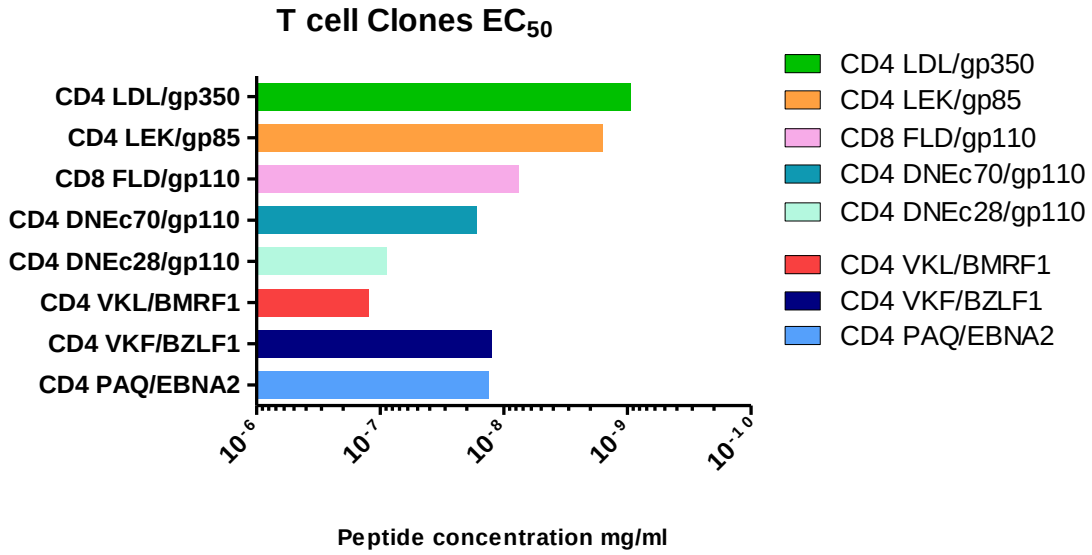

Figure 10. EC50 values of IFNγ response by T cell clones, indicating relative avidity of the clones. Groups of clones LDL/LEK, FLD/DNEc70/VKF/PAQ and DNEc28/VKL have similar avidities.

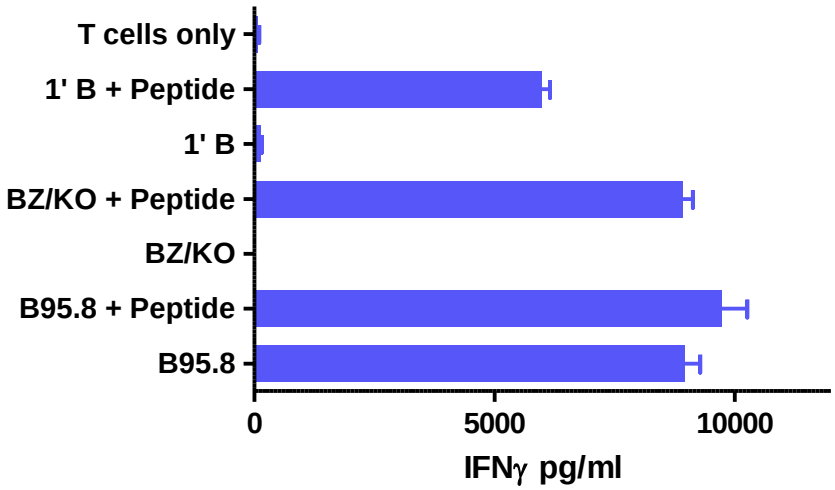

Figure 11. T cell IFNγ control assay. Performed in conjunction with each experiment to confirm ability of B cells to present target epitope and T cells to respond. Here, LDL specific CD4 T cell recognition of target viral peptide (gp350) is functional in both BZLF K/O LCLs and primary B cells with response activation detectable by IFNγ.

3.5 Antigen presentation early after EBV infection

Initial experiments were designed to assess the ability of infected B cells to present viral envelope proteins delivered as components of the incoming virion. BZLF1 knockout LCLs – with no lytic protein expression – were used as a control, as these cells are activated and efficient antigen presenters.

Infection of BZLF1 knockout LCLs is associated with rapid processing of viral coat antigens and detection of presented antigen on the surface via HLA class II within 3 hours post-binding. Presentation peaked following 5 hour incubation and reached a plateau shortly after. In contrast T cell recognition of infected primary B cells was not seen up to 7 hours post-binding, but could be detected after 18 hours if the target cells were left unfixed before addition to the assay (Figure 11).

Fixation reduces recognition of presented antigens and explains the disparity between the 7 hour and 18 hour time-points in LCLs. Importantly, a T cell response to antigen

presentation via primary B cells is observed indicating that the minimum timescale for response lies somewhere between the 7 and 18 hour time-points. Importantly, secretion of IFNγ requires *de novo* transcription and total time from T cell antigen recognition to IFNγ production is approximately 8 hours. Therefore T cell detection of antigen presented via the B cells in the unfixed 18hr time-points must occur before 10 hours post binding to allow for IFNγ production.

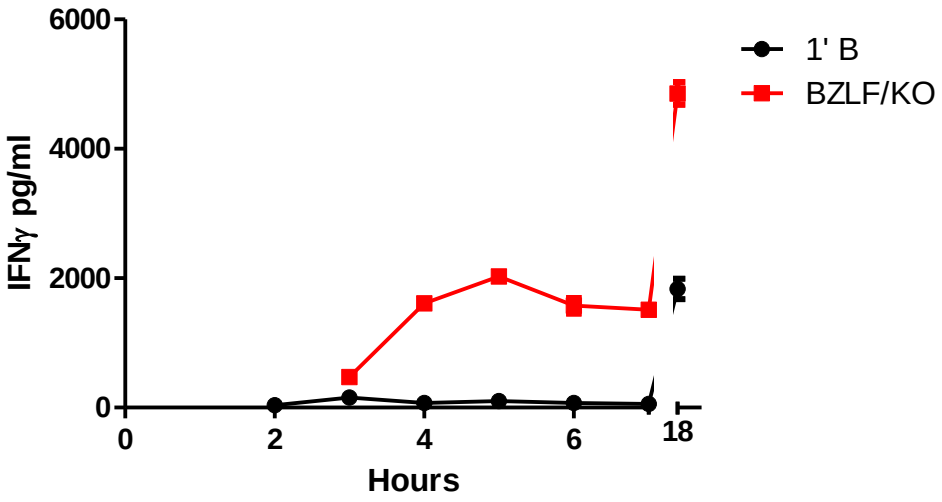

Figure 12. Antigen processing and presentation of LDL/gp350 epitope by primary B cells and BZLF knockout LCLs. Presentation in LCLs is rapid with first indication at the 3 hour time-point reaching peak at 5 hours with plateau following. In contrast primary B cells do not present before 7 hours, but have by 18 hours post-binding. Note that samples taken to 18 hours were unfixed.

3.6 EBV infected primary B cells present virion antigens within 7hrs

We therefore repeated the infection assay over an extended 12 hour timescale (Figure 13). This confirmed previous results showing T cell recognition of infected LCLs from 3 hours post-binding and additionally demonstrated recognition of primary B cells from 7 hours post binding by both gp350 and gp85 specific CD4+ T cells. As previous results showed no recognition up to the 7 hour time-points for this experiment were selected to cover post-7 hours more completely and so no 6 hour time-point data is available. Taken

together with previous results it is suggested that virion antigens can be presented to CD4+ T cells near to this 7 hour time-point post-binding.

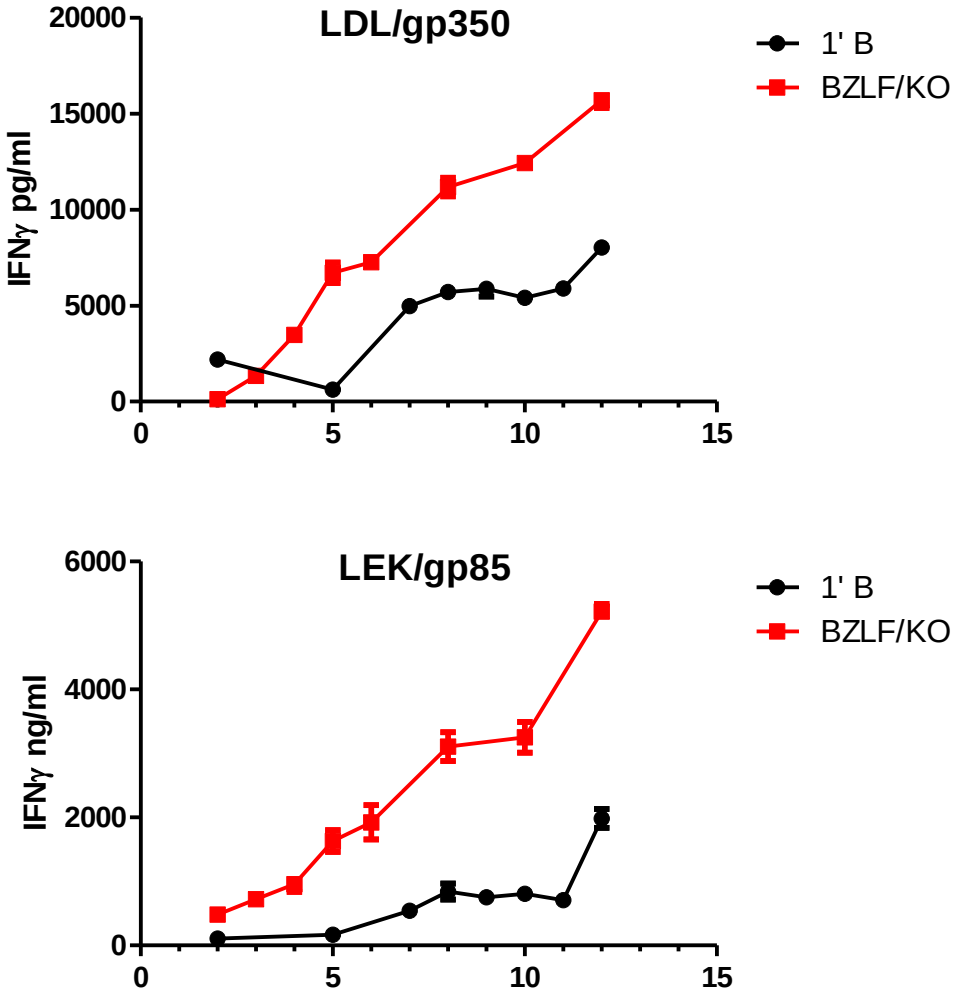

Figure 13. Antigen processing and presentation of LDL and LEK epitopes by primary B cells and BZLF knockout LCLs over 12 hour time-course. Presentation in primary B cells occurs at 7 hours.

3.7 Viral entry is required for early CD4+ T cell recognition

In order to establish whether T cell responses to virus peptides required receptor-mediated uptake 1'B cells were infected in parallel with knockout gp350 virus and wild type virus at equivalent MOI of 100. In both LCL and primary B cells presentation of viral peptides (gp85, gp350) was observed in the wild type virus. However, no T cell

responses were observed to LCL or primary B cells infected with knockout virus lacking cell binding glycoprotein gp350 (Figure 14).

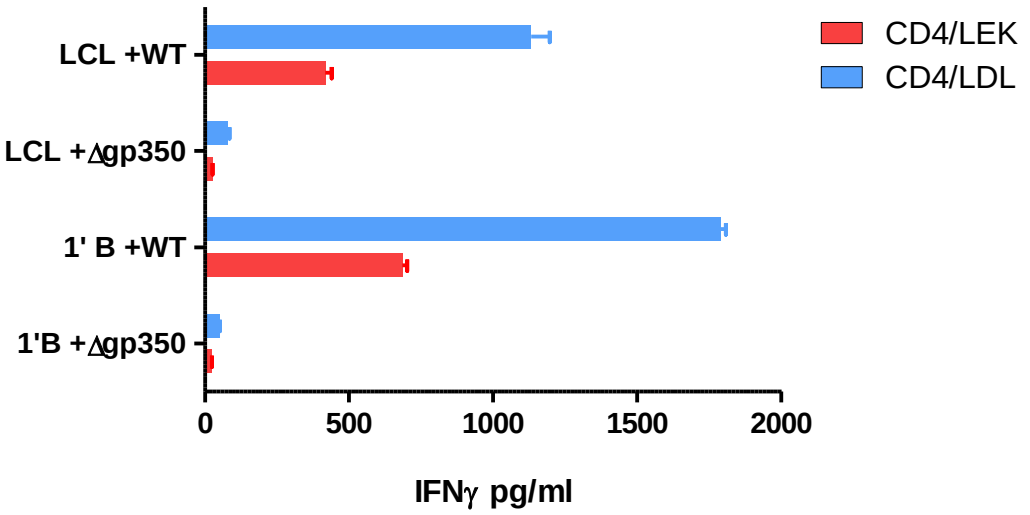

Figure 14. Responses of LEK/LDL specific CD4+ T cells to gp85 and gp350. Responses are seen to peptide, but absent to infection with gp350 knockout

3.8 Viral antigen requires intra-cellular processing for CD4+ T cell recognition

Surface HLA class II molecules are capable of binding and pseudo-presenting peptide from the environment around the cell. In order to establish that the T cell recognition detected is of endosomally processed antigen, an assay was performed in which B and LCL cells were fixed before virus binding. Additionally an equal number of cells were incubated with free peptide solution to confirm that fixation did not impair the capacity of the surface HLA to present peptide. Neither the fixed B cells nor the LCLs exposed to whole virus were able to generate a T cell response (Figure 15), indicating that internalisation of virus is required for the observed T cell responses. Further, this experiment excludes the possibility of free peptide in the virus preparation being responsible for T cell recognition seen earlier.

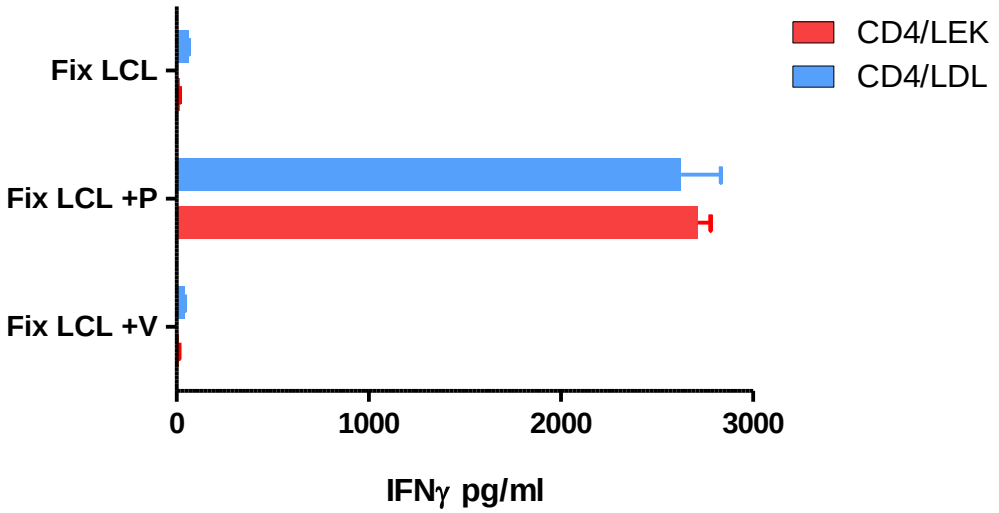

Figure 15. Responses of LEK/LDL specific CD4+ T cells to gp85 and gp350 respectively. Responses are seen to peptide, but absent in fixed cells

3.9 T cell responses are only against capsid antigens

We were interested to see whether virus-borne antigen could be similarly processed for CD8+ T cell recognition by cross-presentation. Further we wanted to confirm that only virus-borne antigen is processed for CD4+ T cell recognition at these early states post-infection, not antigens that require transcription from the EBV genome. In order to further clarify the routes for host recognition of active infection, it was necessary to exclude the possibility of recognition of endocytosed viral antigen via the HLA class I pathway. If antigen from endocytosed virus were presented in this way it would provide a mechanism for recognition of infected B cells by CD8+ T cells prior to active lytic infection. Primary B cells and BZLF K/O LCLs were incubated with wild type virus for 12 hours post-binding. Infected cells were assayed with a range of T cell clones specific for a number of viral proteins, both capsid-borne and proteins requiring transcription from the incoming virus genome. In addition a set of peptide controls were performed to confirm T cell sensitivity to targets.

Responses were only observed to virion borne target epitopes, specifically LDL (gp350) and LEK (gp85) as previously demonstrated (Figure 16). No CD4+ T cell responses were shown to any immediate early, early or latent proteins that are not components of the virus particle. Additionally, no CD8+ responses were observed to virus-borne glycoprotein gp110 indicating that presentation of endocytosed virus does not occur via the HLA class I pathway.

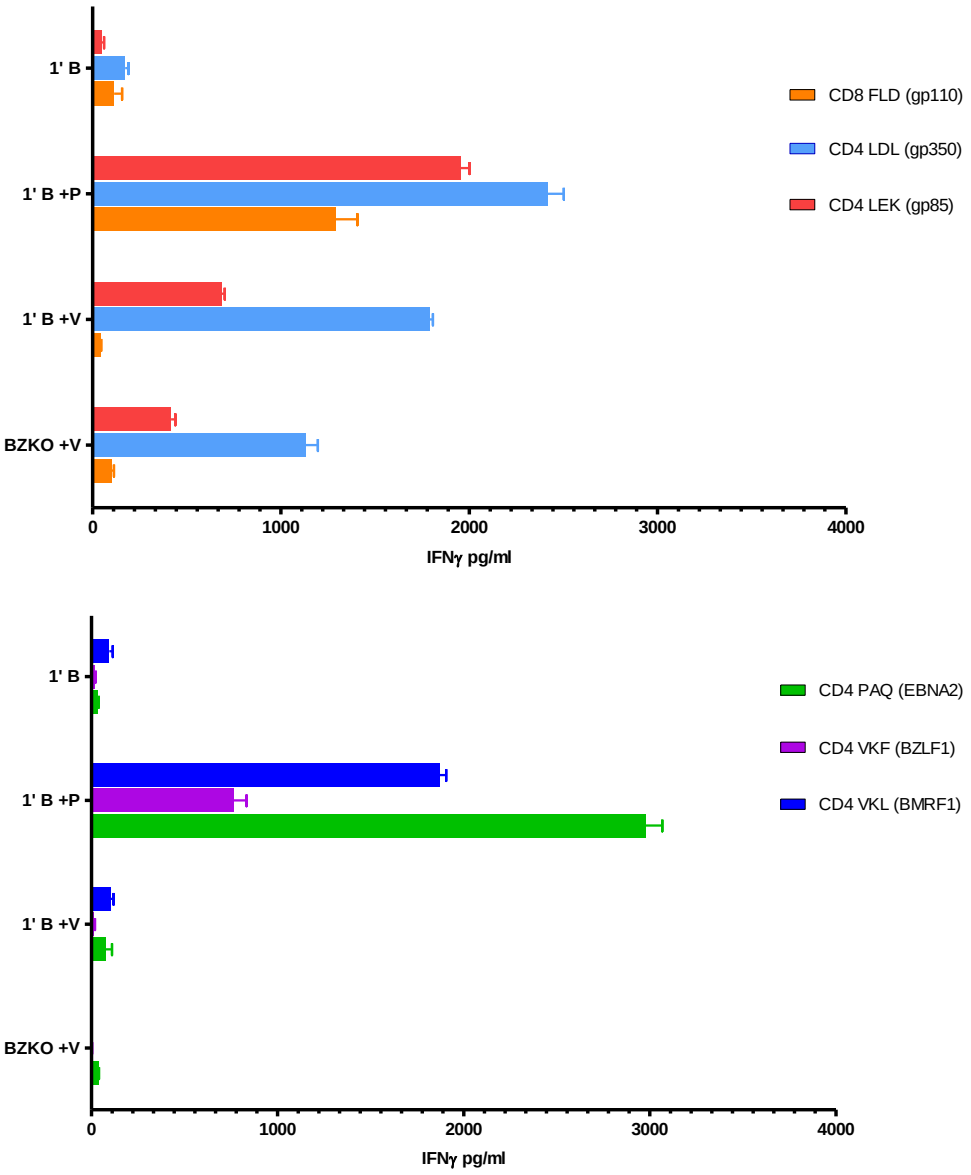

Figure 16. CD4+ & CD8+ T cell responses to early, late and lytic antigens. Responses are only seen to LDL and LEK epitopes from structural virion proteins, not early or immediate early proteins. Further, no response is seen in CD8+ T cells to virion antigen gp110.

3.10 Recognition of glycoprotein knockout virus-infected B cells

To assess the contribution of viral membrane glycoproteins to binding, internalisation, fusion and processing of virus by the host cell, a number of knockout viruses were used in comparative infection assays over a range of MOIs. A brief outline of each glycoprotein knockout is given below, for a full list see Table 2.

- **gp350/220** – Binds CR2/CD21, initial attachment and entry
- **gp85, gp110, gp42** – Form complex, with gp42 binding HLA class II in the endosomal pathway triggering fusion and release of the capsid into the cytosol. May also bind HLA class II on the surface, with possible role in entry.

3.10.1 Recognition of knockout virus-infected B cells by gp350-specific CD4+ T cells

In the first experiment T cell clones specific for gp350 epitope LDL were used to assay presentation of viral antigen following infection with various knockout viruses. As the assay target was for gp350 the absence of a response in the gp350 knockout virus-infected cells is expected, and confirmatory of the status of the knockout virus. The strongest recognition was seen against wild type virus-infected B cells, from physiological MOI of 1 upwards. Knockout viruses gp85 gp42 show much reduced T cell recognition at low MOIs but with increasing recognition at higher levels (Figure 17). Additionally, while gp42 and gp85 knockout viruses share similar profiles at MOIs of 1 and 5, recognition of Δgp85 virus relatively increased from an MOI of 50 and above.

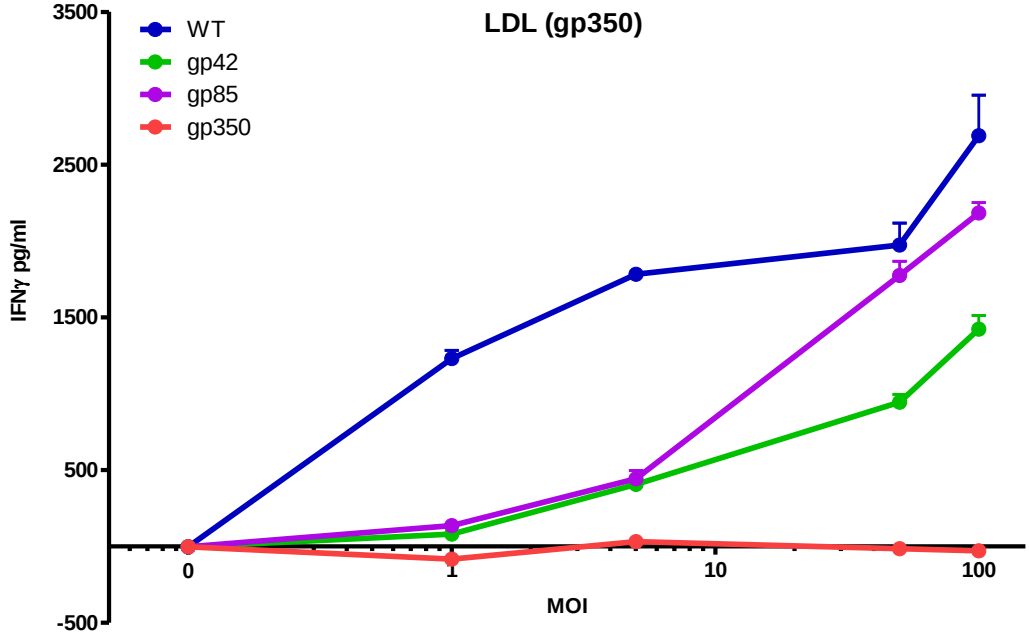

Figure 17. IFNγ responses by CD4+ T clones targeting gp350 epitopes. Complete absence on response by LDL (gp350) specific T cells to Δgp350 virus is observed confirming knockout. At physiological MOIs both Δgp42 and Δgp85 result in similar reduced recognition profile compared to wild type. At higher MOIs reduction in Δgp85 is overcome.

3.10.2 Recognition of knockout virus-infected B cells by gp85-specific CD4+ T cells

As with results for gp350 epitope LDL, recognition of gp85 by the LEK-specific CD4+ T cells is notably higher in wild type virus-infected B cells, albeit with recognition first observed from an MOI of 5 or more (Figure 18). However, gp85 specific T cells show little to no recognition of Δgp42 or Δgp350, with background activation observed in the case of Δgp85 forming the baseline.

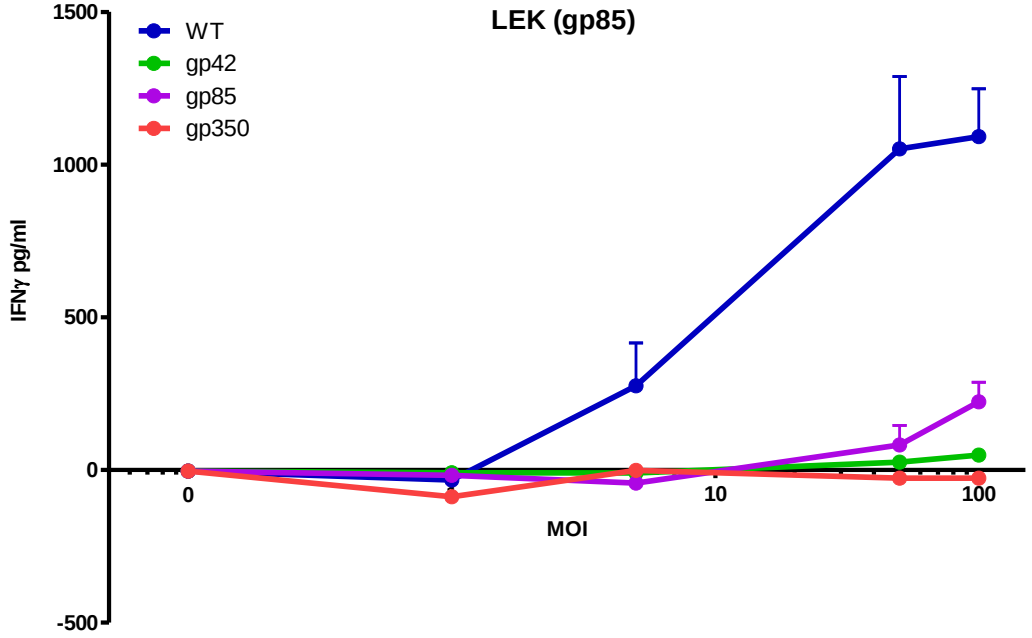

Figure 18. IFNγ responses by CD4+ T clones targeting gp85 epitopes. All knockout viruses exhibit similar profile of little or no recognition by gp85 specific T cells, probably reflecting relative quantities of gp85 in the virion and presentation efficiency.

3.10.3 Recognition of knockout virus-infected B cells by gp110-specific CD4+ T cells

In both of the previous assays T cell target epitopes were within one of the antigens knocked out in one of the viruses used. Here the target epitope DNE gp110 is available to be presented in each of the knockout viruses. Two clones c28 and c70 targeting the epitope were used due to low levels of recognition observed in the T cell avidity assay (Figure 19). As previous results show, recognition of peptides from the wild type assay is detectable from an MOI of 1 (c70). Recognition in Δgp85 virus was only slightly hindered achieving similar levels as that observed in the wild type by MOI of 100. As gp42's established role is as a co-partner with gp85 in the fusion complex, a similar pattern for knockout of these two proteins was expected. However, interestingly Δgp42 and Δgp350 instead show strikingly similar recognition profiles, suggesting that uptake and processing is similar between these two knockouts. At physiological levels of 1+5 MOI the K/O viruses have similar effects. Higher T cell recognition seen at larger MOIs may be due to non-specific endocytosis.

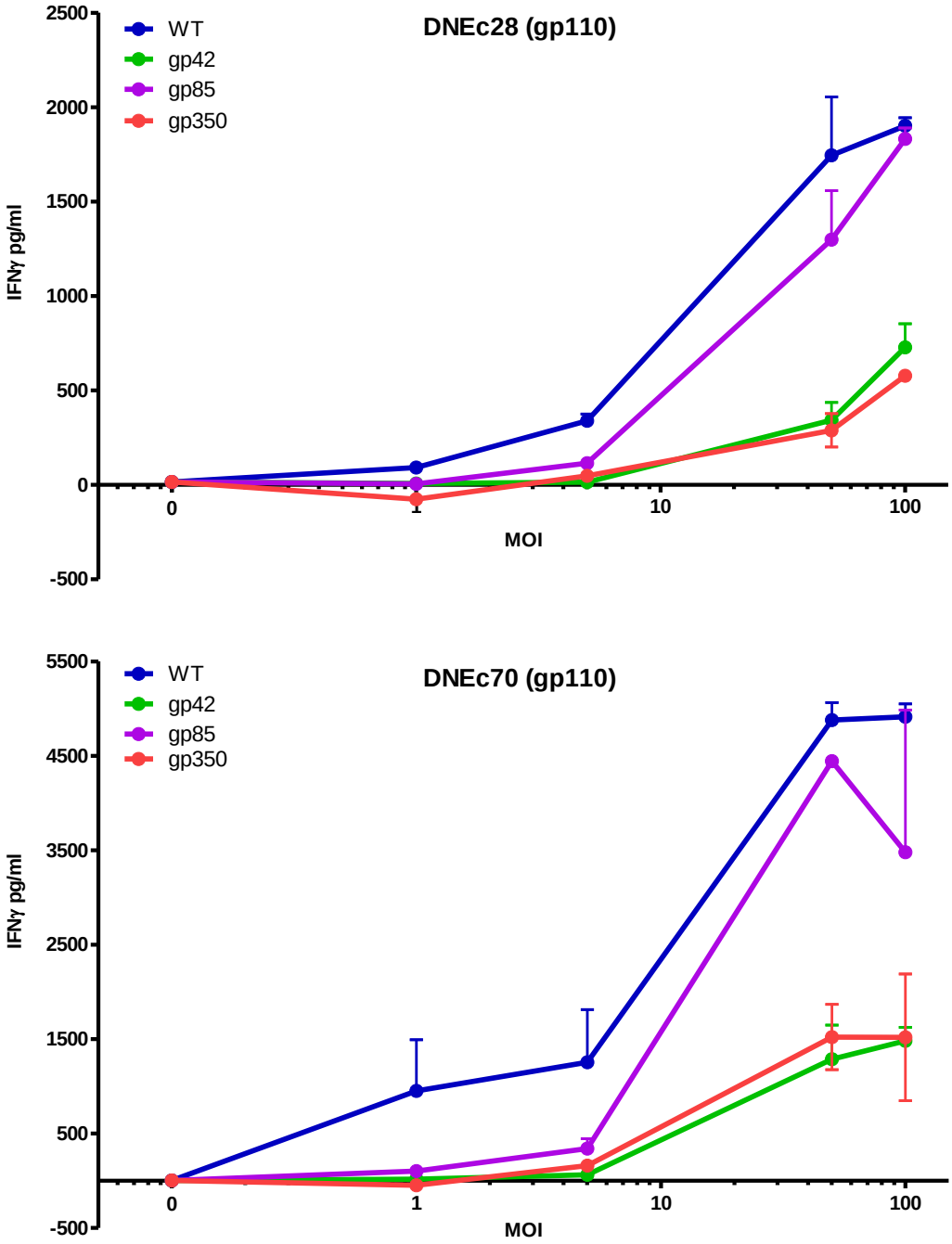

Figure 19. IFNγ responses by CD4+ T clones targeting gp110 epitopes. Note that none of the knockout viruses are for gp110, therefore responses directly reflect uptake and presentation of each virus variant by the primary B cells. Both Δgp42 and Δgp350 share similar profiles, demonstrating uptake at non-physiological MOIs. As previously Δgp85 mimics other knockouts at physiological MOIs but recovers as virus quantity increases.

4 Discussion

Epstein-Barr virus is an endemic virus[1] that has been implicated in a variety of lymphomas and solid tumours human tumours, including Hodgkin's lymphoma (HL) and nasopharyngeal carcinoma[3]. Despite this prevalence, relatively little is known about the early stages of virus infection or the role of virion-borne glycoproteins in uptake and processing. Additionally, responses in primary and long-term infection have been well characterised[24,20] the extent of CD4+ and CD8+ T cell recognition in the early hours following infection of resting B cells is not yet known.

4.1 Endocytosis and trafficking of EBV in primary B cells

The process of endocytosis and trafficking of EBV in primary infected B cells is poorly characterised. Here we have used confocal microscopy to obtain an overview of EBV entry and develop representative timeline of EBV uptake and trafficking within the infected cell and provide insights into the process of endosomal migration.

4.1.1 Endocytosis is rapid but rare and restricted in primary B cells

Resting primary B cells are endocytically inactive under normal conditions. Here we show that EBV binding induces endocytosis in these cells within 15 minutes of initial binding, with subsequent co-localisation with early and late endosomes by 30 minutes and 1 hour respectively. Previous electron microscopy studies[47] suggest that the virus is released from early endosomes following acidification by 15 minutes post binding, and capsids were observed at the nucleus 60 minutes following infection. However, we have observed virus envelope (gp350) and virus capsid (p18) in late endosomes. We propose that during fusion and release of the capsid, membrane glycoproteins remain in the internal wall of the endosome. We have also demonstrated that delivery of EBV genomes to the B cell nucleus is extremely inefficient with the majority of virus retained on the B

cell surface, however, the presence virus capsid in late endosomes therefore confirms that fusion is also not guaranteed. We propose that as super-infection of transformed B cells is possible[48] endocytosis and uptake may follow a bi-phasic pattern, with post-uptake inhibition driven by loss of actin cytoskeleton required for the endocytic process.

4.1.2 Endocytosed virus is successfully trafficked endosomally

Trafficking through the early endosomal compartment is a rapid process, and subsequent entry to the late endosomal compartment was observed from 60 minutes post-binding, suggesting efficient endosomal processing particularly for a resting primary B cell. The late-endosomal localisation of EBV in infected primary B cells remained until 2 hours post-binding, although some hints of fusion were seen. Quantification was difficult due to the low quantity of virus entering the primary resting B cell. We can increase sensitivity by generating a recombinant virus expressing fluorescently-labelled structural protein or glycoprotein such as gp350. If coupled with real-time microscopy this could also overcome the technical limitation of using time points in a dynamic system.

4.2 Virion-derived antigens mediate T cell recognition of newly infected B cells

The ability of T cells to recognise and kill newly-infected cells is central to effective clearance of a replicating virus *in vivo* by interrupting the process of replication and spread within the host. Characterising which T cells are able to function in this capacity in the context of EBV has important implications for both vaccine development and adoptive transfer T cell therapy for EBV malignancies[49].

As previously described, EBV infects B cells that constitutively express MHC class II and EBV-specific CD4+ T cells that directly recognise EBV-infected B cells are well

known[25,50]. As EBV infects through endosomal entry the cell is perfectly positioned to process and present the invading virion antigen for presentation by HLA class II in immediate stages of infection. Structural antigen-specific CD4+ T cells may be the first cells of the immune system able to recognise infected cells. Importantly, this processing and presentation would be independent of virus transcription or replication, and performed on the intact virus particle prior to un-coating. As such no viral immune evasion genes would be able to be transcribed and no capsid-borne host regulators can be employed – the virus is at its most vulnerable to any defences the host may mount. Such recognition has been demonstrated previously in a limited study[50], but only 24 hours post infection, Therefore, we here study CD4+ and CD8+ T cell recognition immediately post-infection.

4.2.1 Response is to HLA-II processed competent infective virus

We first excluded other potential routes for viral antigen uptake and subsequent presentation, demonstrating through gp350 knockout and fixed cells that presentation of virion-borne antigens to CD4+ T cells was dependent on receptor-mediate virus entry and did not occur via non-specific processing of antigen. Recognition of structural viral antigens presented via the HLA class II pathway to HLA matched specific CD4+ T cells was rapid following initial binding. CD4+ T cell recognition of viral epitopes presented by infected endocytically active LCLs occurred at just 3 hours post-binding. In dormant 1°B cells initial T cell responses were observed at 7 hours post-infection, still remarkably early. In conjunction with previous results a broad timeline may be established for the uptake and presentation of viral antigen as described in Table 7. Interestingly, after the 8 hour time-point no further increase in CD4+ T cell IFNγ response is seen, adding weight to earlier observations of phasic entry.

Min	Process
0	Endocytosis
15	Early Endosome
60	Late Endosomes & Lysosomes
480	Presentation of HLA class II loaded antigen at 1° B cell surface

Table 7. Putative timeline of endocytosis and endosomal processing in 1° B cells

Importantly, this demonstrates that viral structural-antigen T cell clones are able to recognise and respond to infected primary B cells from 3 hours post-binding of the virus particle on the surface of the cell. Given recent demonstrations that some lytic antigen-specific CD4+ T cells can directly kill antigen-expressing B cells *in vitro*[50,21] this suggest a role for structural antigen-specific CD4+ T cells in the early phase of response to *de novo* infection of primary B cells.

However, CD8+ T cells also play a key role in the targeted killing of virally infected cells. In order to clarify the mechanism of early host-recognition, we considered the possibility of both cross-presentation of endocytosed post-fusion viral antigen via the HLA class I pathway. Here we have successfully demonstrated that envelope antigen is not processed for MHC class I presentation. However, the possibility remained that membrane-bound envelope antigens may be excluded by remaining internal to the endosomal compartment following fusion. However, unpublished data colleagues have shown that recognition of other viral antigens including minor capsid p18 requires gene transcription and takes several days to occur.

4.2.2 No responses to immediate-early or early genes

Immune recognition of viral antigens is a central plank of immune responses to infection. In order to minimise their exposure, and therefore limit the ability of the host to mount an effective immune response, many viruses employ a variety of host evasion and control mechanisms[51]. EBV itself contains a number of viral immune evasion proteins including two that act on the HLA class II pathway BZLF1 and gp42[52]. However,

production of these evasion products is dependent on transcription of the viral genome. The earlier a virus is able to initiate transcription of these products the higher the opportunity for survival.

Using an assay of epitopes to immediate early, early and lytic viral gene products, we confirmed that no such viral replication was taking place with experimental timescales. Only structural viral proteins gp85, gp110 and gp350 were detectable by CD4+ T cell assay by 12 hours post-binding suggesting CD4+ T cell recognition of structural virion antigens is the key mechanism for recognition of early infected B cells. Further, it is proposed that CD4+ T cell mediated targeted cell killing may have a key role in control of early or reactivating infections *in vivo*.

4.3 The role of EBV glycoproteins in viral entry

Envelope glycoproteins play a central role in the EBV infectious process and individual roles of some glycoproteins are well characterised. The initial attachment of EBV to the B cell is mediated via the high affinity interaction between gp350/220 and CR2 (CD21)[27]. Subsequent interaction between gp42 and HLA class II, followed by the recruitment of gp85 and gp25 forms a tripartite complex. Either interaction of gp350 with CD21, interaction of gp42 with HLA class II or interaction of gp25/gp85 with an as yet unknown fusion receptor induces endocytosis[39]. Our experiments using individual glycoprotein knockouts and the highly-sensitive T cell recognition assays have provided further insights as to which interactions induce endocytosis.

4.3.1 Knockout of gp350 inhibits virus binding

As previously described[29], we confirmed that loss of gp350 from the viral envelope prevents viral uptake at physiological multiplicity of infection (MOI) but that low level uptake is present when MOI reaches non-physiological levels (50+) as detected by CD4+

T cells specific to gp110 epitopes. Recognition of gp85 was absent event at these MOI levels, perhaps related to relative quantities of glycoproteins in the viral envelope. However, when taken in the context of the strong response observed in wild type assays at an MOI of one, uptake in the absence of gp350 must be exceptionally low, confirming its key role in specific uptake.

It has been suggested that non-specific uptake may occur via minor ligands and constitutive endocytic activity in the target cells[29], however our earlier confocal microscopy confirmed that resting primary B cells are endocytically inactive prior to infection, suggesting that some trigger or uptake mechanism may be required. Low-affinity binding of alternate glycoproteins is one such possibility, e.g. gp42 binds MHC class II in the endosomal pathway[39] and a similar interaction may provide an attachment on the surface of the cell. Such alternative routes for entry may have implications for rare *in* vivo infection of cells of non-B non-epithelial lineage implicated in T cell lymphomas[8], therefore further characterisation is essential.

4.3.2 Knockout gp42 mimics gp350; suggested role for gp42 in entry

The fusion complex of which gp85 is a part interacts with gp42 to enable binding to HLA class II. Therefore, it was expected that knockout of gp42 would produce similar results to those seen for gp85. However, knockout of gp42 resulted in an assay profile mimicking that seen for gp350 across all MOIs – including a complete absence of recognition at physiological levels. As previously described gp350 binds CR2 on the cell surface and gp42 is known to interact with HLA class II[46]. Therefore, these results strongly suggest that gp42 is essential to trigger endocytosis of bound virus – although this must be confirmed by confocal microscopy.

4.3.3 Knockout of gp85 decreases recognition; similar to gp42

As part of the gp45gp25gp85 complex gp85 has a central role in the process of endosomal fusion and loss is associated with a failure to infect[41] either by defects in uptake or fusion. If defects in uptake predominate, knockout was expected to be associated with a *reduction* in subsequent recognition by CD4+ T cells. Conversely, if knockout of gp85 inhibits fusion, it was expected that levels of recognition would be *increased* due endocytosed virus remaining in the endosomal compartment for processing and presentation. In fact, our experiments showed a *decrease* in recognition of viral peptides following gp85 knockout, when compared to that of wild type, similarly to gp42 and gp350 knockout at physiological MOIs.

This strongly suggests a role for gp85, likely as a component of the tripartite complex, in induction of endocytosis. As the ligand for gp85 is currently unknown, further work is needed to characterise the role of this interaction in uptake. However, the possibility of inside-out signalling via an integrin or other molecule, offers an attractive solution to the mechanism of both induced endocytosis and perhaps biphasic entry.

4.4 Conclusions

A number of outstanding questions remain in our understanding of the role of glycoproteins in EBV uptake by primary B cells. However, we have demonstrated that uptake is a rapid, yet selective process, restricted potentially by not just gp350 but other glycoproteins in the virus envelope in as yet unknown interactions. Endocytosis results in rapid and profound up-regulation of endocytic activity in resting primary B cells, yet uptake appears to follow a phasic pattern, with little or no secondary uptake observed during the first 2 hours. Trafficking of endocytosed virus is rapid, reaching the late endosomal compartment within 1 hour. Antigen processing, loading onto HLA class II and presentation at the cells surface occurs within 8 hours of the virus binding on the

cell surface. Such early-warning of cellular infection, well in advance of viral genome transcription, provides an attractive target for immunotherapy.

Fusion within the endosome is far more complex than the gp42/25/85 system outlined here. It has been shown that gp110 is required for endosomal exit[53], and viral tegument protein BNRF1 also has a role with loss resulting in a 20-fold reduction in escape[54]. In all EBV has one of the most complex systems of entry and escape from the endocytic pathway. Therefore to pick this apart, we need several systems ranging from real time confocal microscopy and fluorescently-labelled virus particles, electron microscopy, antibody generation to identify nascent and fusion-competent glycoproteins and a read-out such as the exquisitely sensitive T cells. Until we understand exactly how the virus enters the individual cell types and the role of the viral glycoproteins, we cannot hope to generate an effective vaccine. In patients with EBV lymphoproliferation, these studies will further help us to understand how to best target CD4+ T cell immunotherapy.

References

1. Liao, J.B. Viruses and human cancer. *Yale J Biol Med* **79**, 115-122 (2006).
2. Papesch, M. & Watkins, R. Epstein-Barr virus infectious mononucleosis. *Clin Otolaryngol* **26**, 3-8 (2001).
3. Fields, B. *Fields virology*. (Wolters Kluwer Health/Lippincott Williams & Wilkins: Philadelphia, 2007).
4. Cohen, J. Epstein-Barr virus nuclear protein 2 is a key determinant of lymphocyte transformation. *PNAS* **86**, 9558-9562 (1989).
5. Küppers, R. B cells under influence: transformation of B cells by Epstein–Barr virus. *Nat Rev Immunol* **3**, 801-812 (2003).
6. Fafi-Kremer, S. et al. Long-Term Shedding of Infectious Epstein-Barr Virus after Infectious Mononucleosis. *J INFECT DIS* **191**, 985-989 (2005).
7. Hopwood, P. The role of EBV in post-transplant malignancies: a review. *Journal of Clinical Pathology* **53**, 248-254 (2000).
8. Young, L.S. & Rickinson, A.B. Epstein–Barr virus: 40 years on. *Nat Rev Cancer* **4**, 757-768 (2004).
9. Guerreiro-Cacais, A.O. Capacity of Epstein-Barr virus to infect monocytes and inhibit their development into dendritic cells is affected by the cell type supporting virus replication. *Journal of General Virology* **85**, 2767-2778 (2004).
10. Steven, N.M., Leese, A.M., Annels, N.E., Lee, S.P. & Rickinson, A.B. Epitope focusing in the primary cytotoxic T cell response to Epstein-Barr virus and its relationship to T cell memory. *J. Exp. Med* **184**, 1801-1813 (1996).
11. Callan, M.F. et al. Direct visualization of antigen-specific CD8+ T cells during the primary immune response to Epstein-Barr virus In vivo. *J. Exp. Med* **187**, 1395-1402 (1998).
12. Catalina, M.D., Sullivan, J.L., Brody, R.M. & Luzuriaga, K. Phenotypic and functional heterogeneity of EBV epitope-specific CD8+ T cells. *J. Immunol* **168**, 4184-4191 (2002).
13. Bihl, F. et al. Impact of HLA-B alleles, epitope binding affinity, functional avidity, and viral coinfection on the immunodominance of virus-specific CTL responses. *J. Immunol* **176**, 4094-4101 (2006).
14. Ouyang, Q. et al. An age-related increase in the number of CD8+ T cells carrying receptors for an immunodominant Epstein-Barr virus (EBV) epitope is counteracted by a decreased frequency of their antigen-specific responsiveness. *Mech. Ageing Dev* **124**, 477-485 (2003).
15. Steven, N.M. et al. Immediate early and early lytic cycle proteins are frequent targets of the Epstein-Barr virus-induced cytotoxic T cell response. *J. Exp. Med* **185**, 1605-1617 (1997).
16. Murray, R.J. et al. Identification of target antigens for the human cytotoxic T cell response to Epstein-Barr virus (EBV): implications for the immune control of EBV-positive malignancies. *J. Exp. Med* **176**, 157-168 (1992).
17. Hislop, A.D., Taylor, G.S., Sauce, D. & Rickinson, A.B. Cellular Responses to Viral Infection in Humans: Lessons from Epstein-Barr Virus. *Annu. Rev. Immunol.* **25**, 587-617 (2007).
18. Amyes, E. et al. Characterization of the CD4+ T cell response to Epstein-Barr virus during primary and persistent infection. *J. Exp. Med* **198**, 903-911 (2003).
19. Maini, M.K., Gudgeon, N., Wedderburn, L.R., Rickinson, A.B. & Beverley, P.C. Clonal expansions in acute EBV infection are detectable in the CD8 and not the CD4 subset and persist with a variable CD45 phenotype. *J. Immunol* **165**, 5729-5737 (2000).

20. Precopio, M.L., Sullivan, J.L., Willard, C., Somasundaran, M. & Luzuriaga, K. Differential kinetics and specificity of EBV-specific CD4+ and CD8+ T cells during primary infection. *J. Immunol* **170**, 2590-2598 (2003).
21. Long, H.M. et al. Cytotoxic CD4+ T cell responses to EBV contrast with CD8 responses in breadth of lytic cycle antigen choice and in lytic cycle recognition. *J. Immunol* **187**, 92-101 (2011).
22. Bickham, K. et al. EBNA1-specific CD4+ T cells in healthy carriers of Epstein-Barr virus are primarily Th1 in function. *J. Clin. Invest* **107**, 121-130 (2001).
23. Pudney, V.A. CD8+ immunodominance among Epstein-Barr virus lytic cycle antigens directly reflects the efficiency of antigen presentation in lytically infected cells. *Journal of Experimental Medicine* **201**, 349-360 (2005).
24. Adhikary, D. et al. Immunodominance of Lytic Cycle Antigens in Epstein-Barr Virus-Specific CD4+ T Cell Preparations for Therapy. *PLoS ONE* **2**, e583 (2007).
25. Taylor, G.S. et al. A role for intercellular antigen transfer in the recognition of EBV-transformed B cell lines by EBV nuclear antigen-specific CD4+ T cells. *J. Immunol* **177**, 3746-3756 (2006).
26. Haque, T. et al. Treatment of Epstein-Barr-virus-positive post-transplantation lymphoproliferative disease with partly HLA-matched allogeneic cytotoxic T cells. *Lancet* **360**, 436-442 (2002).
27. Tanner, J. Epstein-barr virus gp350/220 binding to the B lymphocyte C3d receptor mediates adsorption, capping, and endocytosis. *Cell* **50**, 203-213 (1987).
28. Moore, M.D. et al. Inhibition of Epstein-Barr virus infection in vitro and in vivo by soluble CR2 (CD21) containing two short consensus repeats. *J. Virol* **65**, 3559-3565 (1991).
29. Janz, A. et al. Infectious Epstein-Barr virus lacking major glycoprotein BLLF1 (gp350/220) demonstrates the existence of additional viral ligands. *J. Virol* **74**, 10142-10152 (2000).
30. Fingeroth, J.D., Diamond, M.E., Sage, D.R., Hayman, J. & Yates, J.L. CD21-Dependent infection of an epithelial cell line, 293, by Epstein-Barr virus. *J. Virol* **73**, 2115-2125 (1999).
31. Sixbey, J.W. & Yao, Q.Y. Immunoglobulin A-induced shift of Epstein-Barr virus tissue tropism. *Science* **255**, 1578-1580 (1992).
32. Tugizov, S.M., Berline, J.W. & Palefsky, J.M. Epstein-Barr virus infection of polarized tongue and nasopharyngeal epithelial cells. *Nat. Med* **9**, 307-314 (2003).
33. Shannon-Lowe, C.D. Resting B cells as a transfer vehicle for Epstein-Barr virus infection of epithelial cells. *Proceedings of the National Academy of Sciences* **103**, 7065-7070 (2006).
34. Kaetzel, C.S., Robinson, J.K., Chintalacharuvu, K.R., Vaerman, J.P. & Lamm, M.E. The polymeric immunoglobulin receptor (secretory component) mediates transport of immune complexes across epithelial cells: a local defense function for IgA. *Proc. Natl. Acad. Sci. U.S.A* **88**, 8796-8800 (1991).
35. Molesworth, S.J., Lake, C.M., Borza, C.M., Turk, S.M. & Hutt-Fletcher, L.M. Epstein-Barr virus gH is essential for penetration of B cells but also plays a role in attachment of virus to epithelial cells. *J. Virol* **74**, 6324-6332 (2000).
36. Borza, C.M., Morgan, A.J., Turk, S.M. & Hutt-Fletcher, L.M. Use of gHgL for attachment of Epstein-Barr virus to epithelial cells compromises infection. *J. Virol* **78**, 5007-5014 (2004).
37. Xiao, J., Palefsky, J.M., Herrera, R. & Tugizov, S.M. Characterization of the Epstein-Barr virus glycoprotein BMRF-2. *Virology* **359**, 382-396 (2007).
38. Johannsen, E. et al. Proteins of purified Epstein-Barr virus. *Proc. Natl. Acad. Sci. U.S.A* **101**, 16286-16291 (2004).
39. Spear, P.G. & Longnecker, R. Herpesvirus entry: an update. *J. Virol* **77**, 10179-10185 (2003).

40. Miller, N. & Hutt-Fletcher, L.M. Epstein-Barr virus enters B cells and epithelial cells by different routes. *J. Virol* **66**, 3409-3414 (1992).
41. Miller, N. & Hutt-Fletcher, L.M. A monoclonal antibody to glycoprotein gp85 inhibits fusion but not attachment of Epstein-Barr virus. *J. Virol* **62**, 2366-2372 (1988).
42. Haan, K.M. & Longnecker, R. Coreceptor restriction within the HLA-DQ locus for Epstein-Barr virus infection. *Proc. Natl. Acad. Sci. U.S.A* **97**, 9252-9257 (2000).
43. Wang, X., Kenyon, W.J., Li, Q., Müllberg, J. & Hutt-Fletcher, L.M. Epstein-Barr virus uses different complexes of glycoproteins gH and gL to infect B lymphocytes and epithelial cells. *J. Virol* **72**, 5552-5558 (1998).
44. Neuhierl, B., Feederle, R., Hammerschmidt, W. & Delecluse, H.J. Glycoprotein gp110 of Epstein-Barr virus determines viral tropism and efficiency of infection. *Proc. Natl. Acad. Sci. U.S.A* **99**, 15036-15041 (2002).
45. Borza, C.M. & Hutt-Fletcher, L.M. Alternate replication in B cells and epithelial cells switches tropism of Epstein-Barr virus. *Nat. Med* **8**, 594-599 (2002).
46. Hutt-Fletcher, L.M. Epstein-Barr Virus Entry. *Journal of Virology* **81**, 7825-7832 (2007).
47. Moore, M.D., DiScipio, R.G., Cooper, N.R. & Nemerow, G.R. Hydrodynamic, electron microscopic, and ligand-binding analysis of the Epstein-Barr virus/C3dg receptor (CR2). *J. Biol. Chem* **264**, 20576-20582 (1989).
48. Klein, G., Dombos, L. & Gothoskar, B. Sensitivity of Epstein-Barr virus (EBV) producer and non-producer human lymphoblastoid cell lines to superinfection with EB-virus. *Int. J. Cancer* **10**, 44-57 (1972).
49. Haque, T., McAulay, K.A., Kelly, D. & Crawford, D.H. Allogeneic T-Cell Therapy for Epstein-Barr Virus-Positive Posttransplant Lymphoproliferative Disease: Long-Term Follow-Up. *Transplantation* **90**, 93-94 (2010).
50. Adhikary, D. Control of Epstein-Barr virus infection in vitro by T helper cells specific for virion glycoproteins. *Journal of Experimental Medicine* **203**, 995-1006 (2006).
51. Horst, D. et al. EBV protein BNLF2a exploits host tail-anchored protein integration machinery to inhibit TAP. *J. Immunol* **186**, 3594-3605 (2011).
52. Ressing, M.E. & Wiertz, E.J.H.J. Manipulation of the immune response by Epstein-Barr virus and Kaposi's sarcoma-associated herpesvirus: consequences for tumor development. *Semin. Cancer Biol* **18**, 379-380 (2008).
53. Neuhierl, B. et al. Primary B-cell infection with a deltaBALF4 Epstein-Barr virus comes to a halt in the endosomal compartment yet still elicits a potent CD4-positive cytotoxic T-cell response. *J. Virol* **83**, 4616-4623 (2009).
54. Feederle, R. et al. Epstein-Barr virus BNRF1 protein allows efficient transfer from the endosomal compartment to the nucleus of primary B lymphocytes. *J. Virol* **80**, 9435-9443 (2006).

Do differentiated macrophages display profoundly different metabolic profiles, reflecting their different functions?

Martin Fitzpatrick

A thesis submitted to the University of Birmingham for the degree of

MRES BIOMEDICAL RESEARCH

Supervisors: Dr Stephen Young and Dr Graham Wallace

Table of Contents

Table of Figures

Table of Abbreviations

CD4 Cluster of differentiation 4; T cell receptor co-receptor found on T_h, T_{reg} cells

CD8 Cluster of differentiation 8; T cell receptor co-receptor found on CTLs

CD14 Cluster of differentiation 14; Pattern recognition co-receptor for LPS

CD200 Cluster of differentiation 200; Macrophage lineage inhibitory signal

GM-CSF Granulocyte-macrophage colony stimulating factor

M-CSF Macrophage colony stimulating factor

IL-6 Interleukin 6; pro-inflammatory cytokine

IL-10 Interleukin 10; anti-inflammatory cytokine

LPS Lipopolysaccharide endotoxin surface of Gram -ve bacteria

NMR Nuclear magnetic resonance; nuclear re-emission of energy identifies molecules

PCA Principal component analysis; statistically identifies contributions to variance

Abstract

Macrophages have a wide range of immunological and non-immunological functions in the host, ranging from clearance of apoptotic cells, tissue remodelling, and release of pro and anti-inflammatory mediators at site of tissue damage or infection. Within these wide-ranging functions however, subsets of macrophages show unique phenotypic adaptations to their role. Studies on monocyte-derived cell lines have shown that these phenotypic differences are matched by underlying metabolic signatures, with the potential to have profound effects on cell capabilities. In order to determine whether differentiated macrophages displayed similar profound metabolic profiles, and whether these differences affect function, we differentiated primary blood monocytes under a range of culture oxygenation conditions. Initial results show significant differences in the metabolic profiles of M1 vs. M2 macrophages undergoing differentiation, with M1s displaying much reduced lactate levels, and corresponding increases in glucose suggestive of gluconeogenesis via putative PFKFB3 (fructose-1,6-bisphosphatase) activity. M1s were demonstrated to be constitutively active under reperfusion conditions, with no corresponding metabolic changes following LPS stimulation. M2s, in contrast, showed an expected hypoxia profile of increased lactate levels under differentiation, and remained inactive in reperfusion conditions, however production of IL-10 following LPS stimulation was shown to be significantly reduced in hypoxic conditions. A model of permissive inflammation during M1 infiltration and under hypoxia is suggested, with reperfusion and reduced recruitment driving resolution in normal tissues. However, in persistently hypoxic tissues or regions of aberrant recruitment and proliferation, the potential exists for differentiating macrophages to drive and maintain a chronic inflammatory state.

1 Introduction

1.1 Macrophages

Macrophages are monocyte lineage derived white blood cells, with a role in both non-specific innate immune responses and the initiation of adaptive immunity. In the tissues macrophages have an important role in clearance of pathogens and cellular debris, antigen presentation and immune stimulation and regulation[1].

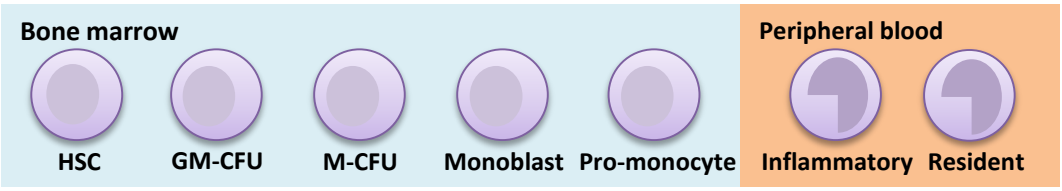

Figure 1. Differentiation and migration of monocytes from bone marrow to the circulation. Adapted from 'Exploring the full spectrum of macrophage activation' D Mosser, J. Edwards. Nat. Rev. Imm. 2008.[2]

Production of PBMCs occurs in the bone marrow from a common myeloid progenitor shared with neutrophils and dendritic cells[1]. Myeloid progenitor cells sequentially differentiate to monoblasts, pro-monocytes, and monocytes. Matured monocytes are then released into the peripheral blood as non-dividing cells, representing about 5-10% of peripheral blood leukocytes[3], and circulating for an average of 3 days before ultimately migrating into the tissues[4]. There is debate about whether sub-populations of macrophages are predefined, or whether subsequent differentiation during circulation drives outcome. However, evidence from animal models has demonstrated that migration can occur throughout the differentiation continuum, and suggests that the resulting phenotype may be determined by timing[5,6].

In humans two broad populations are identified in the circulation, termed classical monocytes and non-classical monocytes[6]. The former are $CD14^{hi}$ CD16- and migrate

from the blood shortly after maturation, differentiating to tissue-resident macrophages or dendritic cells. The latter are CD14+ CD16+ and remain resident in the blood, with a putative role in maintenance of the endothelial lining of blood vessels, and as a reserve for tissue resident macrophages[2,7,8]. Post-migration monocytes undergo further differentiation in response local factors, with GM-CSF in the presence of IL-4 promoting dendritic cell formation and GM-CSF/M-CSF driving differentiation to macrophages[9].

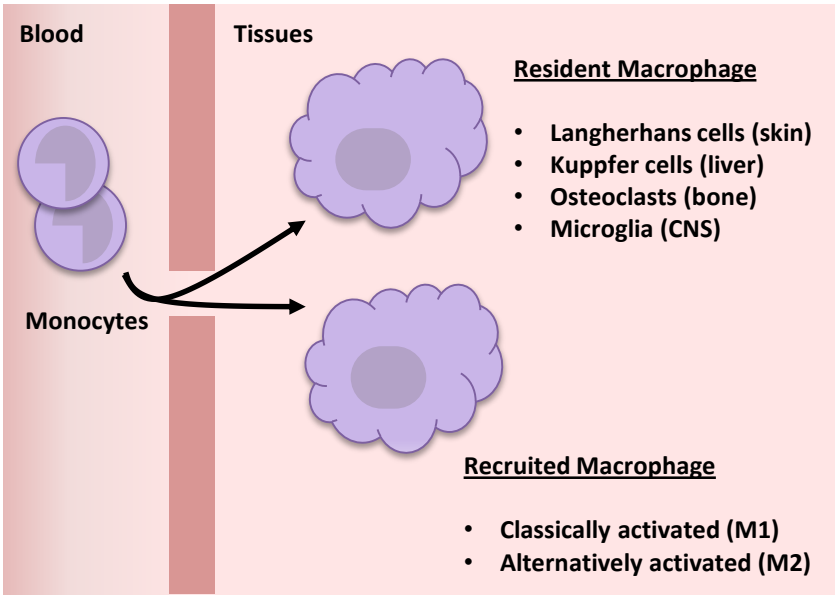

Figure 2. Differentiation and migration of peripheral monocytes to resident tissue macrophages and recruited M1/M2 macrophage populations. 'Alternative activation of macrophages'. Siamon Gordon, Nat. Rev. Imm. 2003[10].

1.2 Macrophage differentiation and activation

Mature populations of recruited macrophages are grouped under two broad classifications defined by phenotypic differences and stimulating cytokines. M1 macrophages, also referred to as 'classically activated' are effector cells, with enhanced microbicidal and tumoricidal effects and secrete pro-inflammatory cytokines[11,2]. M1 macrophages cell-mediated immune responses in the presence of IFNy and TNF with immediate responses are driven by innate NK cells which produce transient high levels

of IFNy in response to stress and infection, while sustained responses follow production of IFNy by T helper 1 (Th1 cells) in an antigen specific manner. However, activated macrophages are also capable of non-specific killing in an antigen-independent manner - and indeed increases antigen availability to local antigen presenting cells.

M2, or 'alternatively activated', macrophages are a less defined family of macrophages, broadly covering any macrophage subtype not stimulated by IFNy but by Th2 type cytokines IL-4 and IL-13[10]. These cells have a role in humoral immunity, repair and vascularisation[12] in damaged tissues, and are therefore associated with the *resolution* of the inflammatory process. IL-4 stimulates arginase activity in alternatively activated macrophages, driving conversion of arginine to ornithine, a key pre-cursor in the production of extracellular matrix[13]. Interestingly, it has recently been shown that the M2 macrophages are able to undergo replication in the tissues, rather than solely migrating from the circulation[14], which may have implications in chronic inflammation.

1.3 Macrophages in the inflammatory site

Differentiated macrophages have important roles in both homoeostasis and control of active infections. Splenic macrophages phagocytose defective erythrocytes, clearing approximately 2 x 10^{11} erythrocytes from the blood each day, recycling 3kg of haemoglobin per year[2]. During tissue remodeling, macrophages are central to the clearance of cells that have undergone apoptosis in the absence of any immune stimulation, via scavenger receptors for phosphatidlyl serine, thrombospondin, integrins and complement[15]. Therefore, the major functions of macrophages are performed in the absence of immune stimulation and without subsequent activation.

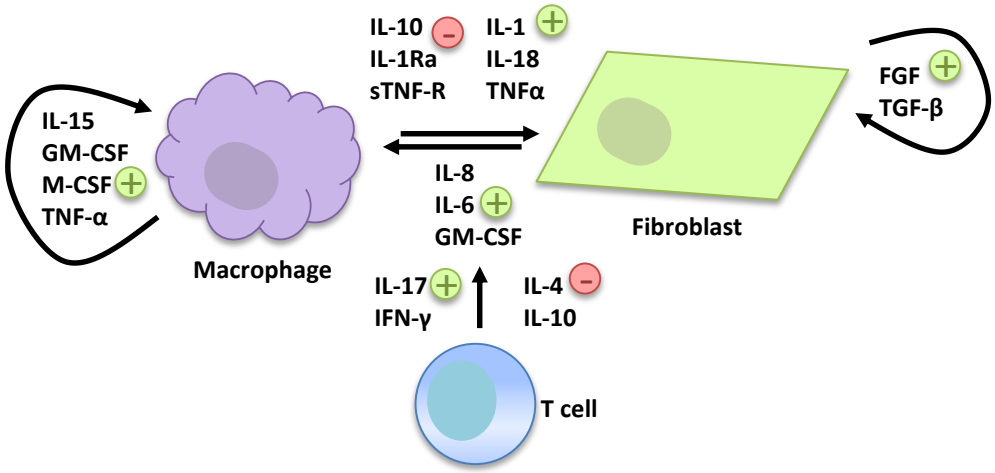

Figure 3. An example inflammatory network from the rheumatoid joint, showing inflammatory and anti-inflammatory cytokine pathways between M1 macrophages, fibroblasts and T cells. Adapted from 'Evolving concepts of rheumatoid arthritis, Firestein GS. Nature 2003[16]

In contrast, necrosis following trauma or infection results in cellular debris high in heat-shock proteins, nuclear proteins, histones and DNA, together with cleaved extracellular matrix components[17]. Subsequent phagocytosis by tissue resident macrophages triggers physiological changes, including surface marker proteins and production of cytokines and pro-inflammatory mediators[2]. Surface TLRs, intracellular PRRs and IL1R on macrophages identify and stimulate responses to danger signals in the surrounding environment, mediated via myeloid differentiation primary-response gene 88 (MyD88)[18]. It has been demonstrated that these responses are present in the absence of adaptive immune co-stimulation[19]. Responses to innate immune stimulation are typically broad but transient, with responses to adaptive stimulation result in more focused and prolonged alterations in macrophage physiology. Macrophages additionally produce several factors to auto-regulate their own physiology.

Macrophages phagocytose pathogen and cellular debris and presenting foreign antigen to helper T cells via MHC class II to trigger appropriate and specific activation and B cell antibody production. Phagocytosis simultaneously triggers macrophage release of pro-

inflammatory cytokines, central to the recruitment of other immune cells to the site of infection or damage. Activated effector T cells can in turn activate macrophages. Differentiation of immune cells is associated with profound changes in metabolism. For example, T-cell glycolysis is enhanced 6-fold 2 hours following stimulation, and 15-fold 46 hours later[20]. Activation of naïve CD8+ T cells to effector cells induces up-regulation of glycolytic enzyme genes. In turn surrounding environmental metabolic conditions may affect immune cell function, with tumour cell derived lactate supressing proliferation and activation of CD8+ T cells[21]. Likewise, macrophage differentiation is associated with profound changes in cellular metabolism. Similarly, environmental conditions may in turn affect macrophage function.

Tissue injury results in the recruitment of blood monocytes to the tissues and subsequent differentiation, and proliferation, depending on tissue conditions encountered. An initial influx of inflammatory-phenotype M1 macrophages is associated with tissue remodeling and pathogen/particulate phagocytosis. Later, injury-associated hypoxia, anaerobic respiration and resulting high lactate levels drives M2 macrophage pro-angiogenic responses via release of vascular endothelial growth factor (VEGF) in the surrounding tissues. Resident fibroblasts are induced to produce collagen. Resulting reperfusion and a return to tissue integrity drives a reduction in macrophage numbers to normal tissue-resident levels.

1.4 Hypoxia in the inflammatory site

Inflammatory sites are by their nature hypoxic, and such hypoxic sites are a common feature of a number of inflammatory diseases including the synovium of arthritic joins, wounds, bacterial infections and malignant tumours[22]. Local hypoxia develops as the result of either blood vessel occlusion by inflamed tissues, or when existing supply is insufficient for infiltrating or proliferating inflammatory cells. Normal tissue structures

additionally lend themselves to hypoxia, where they are poorly perfused, such as the synovium or eye. Metabolomic analysis of eye fluids from uveitis patients has shown increased levels of oxaloacetate and urea, likely derived from anaerobic respiration by locally activate macrophages[23],[24]. Such metabolites may be indicative of macrophage upregulation of ascorbate transporters[25] reflecting their need to function in inflammatory milieu. However, it is worth noting that not all macrophages are pro-inflammatory, and therefore the presence alone is not indicative of role in disease.

While macrophages are present throughout the tissues of the body, a tendency to accumulate in such areas of hypoxia is suggestive of a role for hypoxic conditions to drive macrophage residence and perhaps activation. Recent studies have shown just such a response, with wide variety of gene expression alterations observed in macrophages exposed to hypoxic conditions. Exposure of macrophages to hypoxic conditions is associated with upregulation of a whole gamut of proinflammatory IL-1[26], IL-6[27], IFN-y[28], TNFa[29]. Conversely it is also associated with upregulation of immunosuppressive genes including PGE2[30], IL-10[28], and downregulation of antigen-presenting CD80[31]. Interestingly, additional angiogenic activity via the upregulation of VEGF and PGDFB[29] suggests a role in both tumor survival and synovial proliferation.

The key step in all both aerobic and anaerobic respiration is the breakdown of glucose to 2x pyruvate and producing 2x ATP in the process. A number of other energy sources may be converted to intermediaries directly including fructose and sucrose.

$$\text{Glucose} + 2\ NAD^+ + 2\ P_i + 2\ ADP \rightarrow 2\ \text{pyruvate} + 2\ NADH + 2\ ATP + 2\ H^+ + 2\ H_2O$$

Under aerobic conditions mitochondrial pyruvate dehydrogenase complex oxidizes pyruvate to acetyl-CoA and CO2 + NADH. This *link reaction* provides the initiation for the

citric acid cycle and subsequent oxidative phosphorylation producing the majority of cellular energy (a maximum of 36-38 ATP/glucose molecule). In contrast, under anaerobic conditions, hypoxia inducible factor HIF-1α induces pyruvate dehydrogenase kinase, inhibiting the conversion of pyruvate to acetyl-CoA in favour of fermentation to lactate[32]. Hypoxia inducible factors (HIFs) are transcription factors activated in response to decreases of oxygen in the cellular environment. A constitutive HIF-1b subunit associates with HIF-1a, 2a or 3a. These alpha-HIFs are extremely short-lived under oxygenated conditions degraded by pVHL. However, hypoxia disrupts pVHL/HIF-a interaction, leading to persistence, interaction with HIF-1b and induction of transcription[33]. Recent studies have shown macrophage expression of HIF-1a in the synovium of rheumatoid arthritis joints, but not in normal or osteoarthritic joints which are not hypoxic[34]. In a mouse model of arthritis, targeted deletion of the HIF-1a gene resulted in a marked reduction of inflammation and macrophage infiltration[32] – strongly suggestive of a role for macrophage responses to hypoxia in rheumatoid arthritis. A possible mechanism of action is shown through the essential role of HIF-1a in the regulation of macrophage glycolysis. Loss of HIF-1a is associated with impaired aggregation, motility, invasiveness and killing of bacteria[32]. Importantly, it has been demonstrated in mouse macrophage cell lines that bacterial LPS is able to stimulate transcription of HIF-1α in the absence of hypoxia[35] – providing an alternate route to these responses.

That such phenotypic changes are observed in response to the hypoxic conditions of the wound site is strongly suggestive of a role for metabolism in regulation of macrophage activity. While normal wound resolution is a tightly regulated process, the presence of long-term inflammatory diseases such as rheumatoid arthritis is indicative of the potential for this regulation to go awry. Sites of chronic inflammation are associated with continued hypoxic, poorly perfused tissues high in lactate, and the associated

activation of tissue-resident macrophages. A preponderance of inflammatory M1 phenotype is also seen, indicative of ongoing inflammatory process. It is unclear whether macrophages are driving or responding to the local tissue conditions, but it is likely that both are occurring. As previously described resolution is dependent on reperfusion and loss of hypoxia, and failure of achieve this may be the driving factor in continued inflammation. However, while the inflamed site exists in a self-maintaining environment, the responsiveness of macrophages to changes in this environment may provide a route to manipulating and ultimately resolving the chronic inflammation. Macrophage responses to hypoxia, and subsequent changes in metabolic profile of the cells may offer targets for intervention – and manipulation of macrophage metabolic pathways, driving respiration via a deactivating or M2-favouring route, may offer a local and well tolerated mechanism of treatment.

1.5 Metabolomics

Metabolomics is a novel systems approach that allows us to address these questions. As transcriptomics involves the study of gene expression, and proteomics the expression of proteins, metabolomics investigates the downstream consequences and phenotypic effects of the activity of these genes and proteins. A hypothesis-forming approach, it starts with analysis of the whole population of small molecular metabolites across the whole population of individuals or samples under study. Data produced may be analysed as-is or frequency binned to reduce the quantity of the data for analysis. Quantification is then performed on peaks, without prior identification, to isolate the peaks or peak collections associated with a particular group of patients, conditions, or cellular profiles. Through this map of metabolites, metabolomics provides a window on the underlying functionality of the system. In studies of patient biofluids access to the metabolome allows integration of patient health and genetic profile with environmental effects to provide a complete picture of the disease state[36] and so aid prediction of

outcome. Repeated sampling allows for understanding of the dynamic processes at work that may differentiate, or predict patient outcomes - perhaps identifying markers in patients for responses to treatment. Such discoveries may prevent unnecessary ineffective intervention, and more rapid, targeted treatments.

These benefits extend to the lab, where the ability to take repeated whole-system measurements of metabolic processes is a valuable method for longitudinal phenotypic analysis. Importantly, the ability to use the same technique to analyse biofluids and cultured cell samples allows for more direct comparisons – and identification of where comparisons fail – informing experimental design.

1.6 NMR spectroscopy

Nuclear magnetic resonance is a phenomenon that may be observed when atoms are subjected to both a static background magnetic field and a secondary oscillating field. Under these conditions interactions between those atoms which possess a 'spin', which may be considered a small magnetic field of their own, interact with the larger fields in a predictable and measurable way.

Spin is a fundamental property of all atomic particles, including electrons, protons and neutrons. Spin quantities are in ½-spin multiples and may be positive or negative. Individual unpaired electrons have a spin of ½, whereas electron pairs (one positive, one negative spin) effectively cancel out the overall observable spin. As such, it is unpaired atomic particles that are detectable and of interest in NMR spectroscopy.

Nuclei	Neutrons	Protons	Unpaired N+P	Net Spin	γ (MHz/T)
^{1}H		1	0+1	1/2	42.58
^{2}H	1	1	1+1	1	6.54
^{31}P	16	15	0+1	1/2	17.25
^{23}Na	12	11	2+1	3/2	11.27
^{14}N	7	7	1+1	1	3.08
^{13}C	7	6	1+0	1/2	10.71
^{19}F	10	9	0+1	1/2	40.08

Table 1. Nuclei commonly used in NMR study

For example, deuterium $_{2}H$, with a single proton, neutron & electron, has a ½ electronic spin, and a nuclear spin of 1. In contrast, helium $_{2}He$, with two neutrons, two protons and two electrons, has a zero electronic and nuclear spin, and as such is undetectable. A list of nuclei commonly used in NMR is shown in Table 1.

The spin of the charged proton creates a magnetic moment vector leading to the proton acting as a small magnet itself. When placed in an external magnetic field the proton aligns with this in either a low energy N-S-N-S or high energy N-N-S-S configuration, and transitions between these states can be induced by photons of equivalent energy. The proportion of spins at high and low energy levels is relative to the temperature of the sample, and as temperature is decreased the majority of spins moves to lower energy state. The signal observed in NMR spectroscopy is relative to the difference between energy absorbed by moving to higher energy states and that released by moving to lower energy states, and therefore to the relative population quantities of each. These interactions, once measured form the basis of the NMR spectroscopy signal

Data produced is in the form of time domain data, and is subsequently processed via Fourier transform (FT) to produce frequency domain data – the frequency peak graph. Molecules have unique, recogniseable patterns of peak frequencies and intensities from which it is possible to derive both the metabolite detected, and in comparison to a known standard, the concentration in the solution. Mapping identified metabolites onto

established metabolic pathways allows for development of regulatory maps, indicating up and down regulation of metabolic enzymes, providing valuable information for further targeted studies.

1.7 Research goals and study methods

The purpose of this study is to test the hypothesis that differentiated macrophages will display profoundly different metabolic profiles that are indicative of function.

Primary blood monocytes will be grown under normoxia (20% oxygen) and hypoxia (1% oxygen) to simulate the conditions likely to be found in inflammatory sites. Effects of this manipulation on the metabolic profiles of the cultured cells may indicate an adaptation to the inflammatory environment or phenotypic change directing alternate function. Differentiation of these monocyte precursors to macrophage and dendritic cells, under different conditions, will be used to demonstrate the effects of environment on underlying metabolic profile. Subsequently cultured cells will be stimulated with LPS to assess the effect of both culture conditions and underlying physiology on response.

2 Materials & Methods

2.1 Culture media & solutions

Culture media	RPMI	500ml
	10% fetal calf serum	50ml
	1% L-glutamine	5ml
	1% Penicillin/streptomycin	5ml

Table 2. Culture media

M1	RPMI + 1% GPS + 10 % Hi FCS	GM-CSF	4ul
M2	RPMI + 1% GPS + 10 % Hi FCS	M-CSF	4ul
DC	RPMI + 1% GPS + 10% Human Serum	GM-CSF	10ul
		IL-4	10ul

Table 3. Primary monocyte differentiation media

Coating buffer (10x stock)	Sodium carbonate	1.36g
	Potassium bicarbonate	7.35g
	- Make up to 100ml H20	
	- Adjust to pH9.2 1M HCl/1M NaOH	
Blocking buffer	PBS	500mls
	Bovine serum albumin	5g
	Tween	250µl
Wash buffer	PBS	5L
	Tween	2.5ml

Table 4. ELISA buffer solutions

40% D_20	60mls
100mM Pi	156ml 2.34g
2mM TMSP	51.6mg
0.08% Azide	120mg
Made up to 150mls with H_2O	

Table 5. NMR buffer solution 1x

2.2 PBMC separation from whole blood

Blood was obtained from donations from apheresis cones obtained from the NHSBT, Birmingham. Blood was diluted in an equal volume of PBS and layered on top of FicollP-Paque. Samples were centrifuged at 1800rpm for 30 minutes at room temperature. The separated PBMC layer was removed, washed twice in 50ml PBS at 1600 and 1200rpm and re-suspended in 10ml RPMI, 1% FCS. The total PBMC count was made and B cell numbers determined by assuming B cells account for 5% of total PBMC.

2.3 Isolation of monocytes from PBMCs

Isolation of monocytes from PBMCs was performed by magnetic activated cell sorting (MACS) as per instructions from Miltenyi Biotec. Briefly, PBMCS were incubates with 80ul MACS buffer per 10^7 cells, and MACS CD14 beads added at 20ul per 10^7 cells for 15 minutes at 4'C. Cells were washed in 1ml MACS buffer per 10^7 cells then resuspended in 500ul MACS buffer per 10^8 cells (5ml/10^7). MACS column was placed in a magnetic field, rinsed through with 3mls MACS buffer solution, and cell suspension was added. Column was washed with 3x 3mls MACS buffer, and run-off collected as waste. Column was transferred to collection tube, with 5ml buffer and syringed to collect cells. Purity of resulting samples was confirmed by flow cytometry.

2.4 Cultured cells from liquid nitrogen storage

Cells were transferred from cryovials into 6ml pre-warmed media in 15ml tube then centrifuged down for 6 minutes at 1200 rpm to pellet. Supernatant media was poured off and cells resuspended in 2mls RPMI+10% FCS then transferred to 25cm^2 flask. Cells were incubated overnight, then transferred to 75cm^2 flask to culture.

2.5 Primary monocyte differentiation

Isolated primary monocytes were seeded at 3x106 cells/well in a 6 well plate, in 4ml media of appropriate type for differentiation (see Table 3). Cultures were incubated for 3 days until initial signs of differentiation and adherence occurred. Supernatant media was removed carefully, avoiding disrupting loose cells, and replaced with 4mls fresh media of the appropriate types. After a further 3 days cells were fully differentiated for stimulation, or assay use.

2.6 Primary monocyte normoxia, hypoxia, reperfusion assay

To assay the metabolic effects of hypoxia and reperfusion on M1, M2 and DCs, these were differentiated as previously described in hypoxic conditions. Media for hypoxic cells was pre-exposed to hypoxic conditions for 1 hour prior to first use, and kept in hypoxic conditions for the duration of the experiment.

At day 3 and day 6 media was removed from cell cultures and frozen down in cryovials for subsequent analysis, and appropriate media for the cultures was replaced. Feeding of hypoxic cells was carried out in the same hypoxic station. Normoxia and reperfusion cells were fed with normoxia-exposed media, with reperfusion cells removed from the hypoxic station for feeding then replaced to re-acclimatise. On day 6 10ng/ml lipopolysaccharide (LPS) was added to half of the cell cultures, and then left overnight. Media was again removed from all cultures to freeze down and remaining cells were retrieved as described below.

2.7 Cell metabolite extraction for metabolomic analysis

All remaining media was removed from the cells via pipette, and cells were washed with 1ml PBS. Adhered cells were air-dried for 15 minutes and then 400ul methanol was added to each well and cells dislodged to solution via cell scraper. Solutions were

pipetted up and down to dislodge cells further and isolate to single cell suspension then transferred to glass vials and placed immediately on dry ice then transferred to -80'C.

The following day glass vials were retrieved from the -80'C. Once defrosted, 325ul pre-chilled distilled H_20 was added to each tube via pipette. Next, 400ul pre-chilled chloroform was added to each tube with a blunt-ended Hamilton syringe and the samples were vortexed for 30 seconds to mix thoroughly. Samples were then transferred to the cold room for 10 minutes to allow phases to separate and then centrifuged at 4'C in swingout rotor at 1200rpm for a further 10 minutes. Once completed, vials were removed from the centrifuge to the bench and left to stand for 5 minutes. The upper (polar) layer 400ul was transferred to eppendorf tubes and stored at -80'C overnight. The following day samples were dried in vacuum dryer for 3-4 hours, and resulting tubes were re-frozed at -80'C until prepared for NMR.

2.8 NMR sample preparation

Samples of 600ul each were prepared from dried cell extract or cell media and aliquoted to eppendorf tubes. 200ul of NMR buffer was added to each sample, to give a final volume of 800ul. Samples were adjusted to pH 7.1-7.2 by addition of 3M HCl (~1ul) then 600ul was loaded to glass NMR tubes and kept at 4'C until required.

2.9 Metabolomic analysis

NMR data collected were phase corrected manually with Bruker XWin-NMR. Bruker datasets were subsequently imported into MatLab and processed using ProMetab v3.3. This performs a number of optimisations, including adjustment to equivalent total surface area, to account for variations in concentration, and log transformation to enable analysis of the full range of detected quantities. Finally, datasets were binned to 0.01ppm bins to reduce the quantity of data for analysis.

2.9.1 Genetic algorithm (Galgo)

Initial process was performed using genetic algorithm Galgo (ref) on exported datasets. A number of scripts were written to automate this process, as well as enabling easier analysis of combinations of classifiers. Briefly, Galgo treats each binned peak as a 'gene', with which it iteratively builds models through a stochastic process. Each model is then used to predict a sample's membership of pre-defined classes. Over a number of generations the relative value of a gene, or group of genes, to describe each sample becomes apparent – and these are identified, rated and output at the end of processing.

Such fitness data can then be used to draw principal-component space maps, identify key metabolites, or test further samples to establish the predictive nature of the model.

2.9.2 Metabolite identification

Metabolites were identified by manual matching of representative, original spectra, against a database of known spectral signatures. Binned spectra were then used to graph relative quantities of metabolites in different samples. Where multiple resonant peaks or peaks spanning multiple bins, exist for metabolites, a summed total of peaks was used to correct for interference from adjacent peaks or signal noise.

Identified quantities were then mapped onto pre-mapped metabolic pathways to attempt to elucidate the implications for cellular respiration and function.

3 Results

3.1 Cell media as an indicator of intracellular metabolism

Metabolite extraction from experiment-terminal cells provides an overview of cellular metabolism at that time only. Using the same technique for timecourse experiments would require large duplication and therefore excessive cell numbers. In order to establish the viability of growth media analysis for metabolomics study we here have performed metabolic analysis of both terminal cell extracts and experimental cell media.

Samples from cell culture at final timepoint of 8 days were analysed by NMR and resulting spectra binned as previously described. Metabolites were identified and relative levels of each metabolite compared as detected by the two methods.

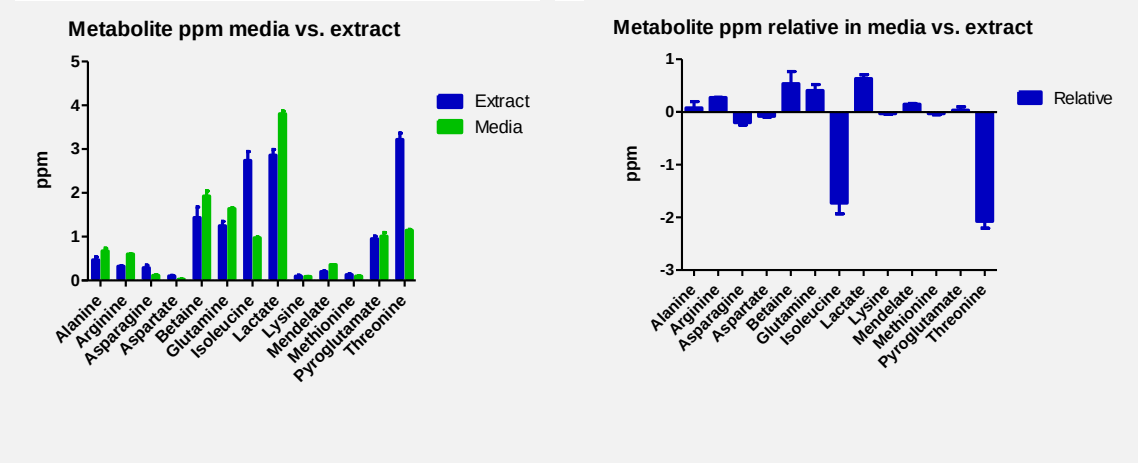

Figure 4. Key metabolites identified by Galgo analysis (see later) here shown at relative levels detected by ppm in media vs. those detected from cell extracts at day 8. Generally a similar profile is observed, with minor variations in quantity except for isoleucine and threonine levels, which are much reduced in media vs. extracts of intracellular metabolites.

Results (Figure 4) show highly similar profiles obtained from analysis of cellular growth media and isolation of metabolites from whole cell extracts, with the notable exception of isoleucine and threonine levels in media significantly lower.

Therefore, it is suggested that cell culture media provide an accurate and representative means to assay cellular metabolic processes in culture, and provide an accurate representation of cellular function. Comparison of relative levels in media must take these differences into account.

3.2 Differentiating monocytes display different metabolic phenotypes

To determine the baseline metabolic differences between M1, M2 and DC cells undergoing differentiation in normal culture conditions cell media were taken from cells at day 3 post-culture under 20% oxygen in cell differentiation media. Media NMR spectra were analysed using Galgo genetic algorithm to identify key metabolite peaks distinguishing the cell types.

Resulting analysis shows that analysis of cell culture media allows full distinction between the three monocyte derived cell cultures, M1, M2 and DCs respectively. Highest identifiable ranking metabolites reported by Galgo are Alanine (ppm 1.5925) and Serine (ppm 3.9625) (Figure 5). As shown in Figure 6 top ranked metabolites do not necessary vary the largest amount, but do so consistently. A full listing of key metabolites identified in this manner is given in Table 6 and Figure 6 with levels of lactate, pyroglutamate, alanine and isoleucine being particularly striking.

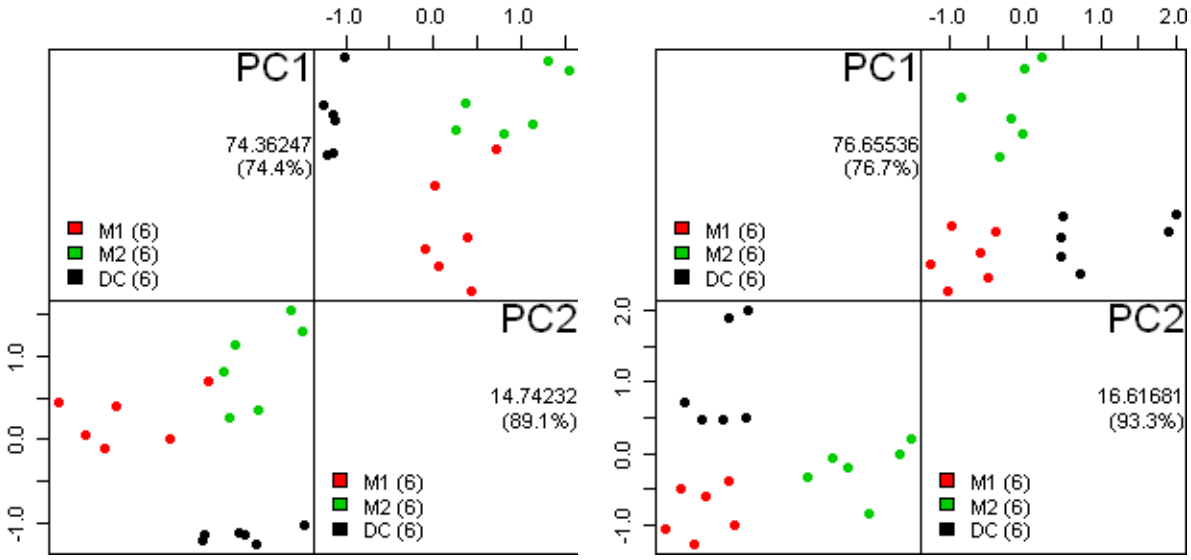

Figure 5. M1, M2, DC (Hypoxia) cell differentiation by two metabolites at timepoint 1 & 2 respectively. Galgo analysis demonstrates full separation of the 3 cell types is possible by the respective levels of just 2 metabolites Arginine (1.5925) and Serine (3.9625).

Ppm	Rank	Metabolite
1.5925	1	Arginine
3.9625	2	Serine
2.4825	3.5	Pyroglutamate
4.1625		
1.6125	5.5	Arginine
2.0625	7	Homoserine
2.0775		
0.9925	8	Isoleucine
1.3025	10	Lactate
3.6875	11	Glucose

Table 6. List of key metabolites identified by Galgo to contribute significantly to differentiating M1, M2, DC profiles during first 7 days. A number of lower-ranked peaks were not identified.

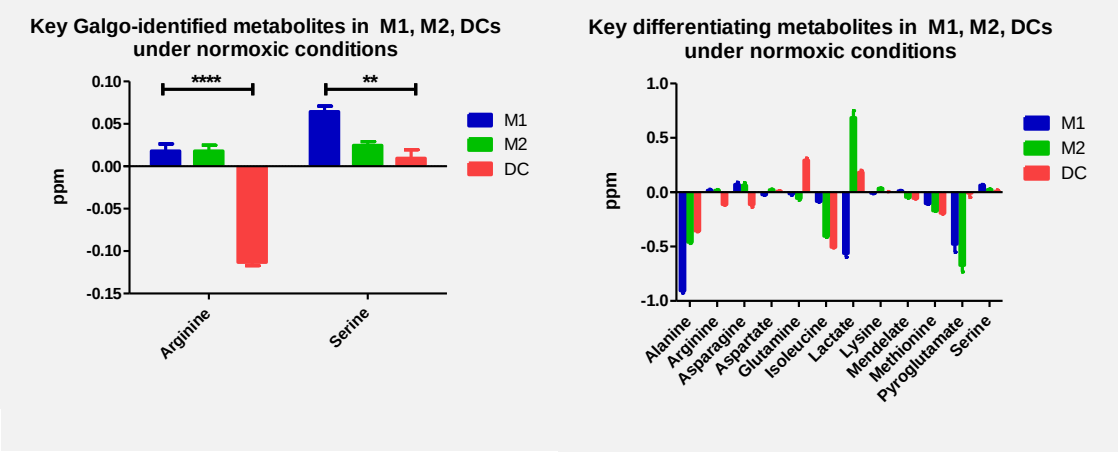

Figure 6. Key metabolites, identified to differentiate M1, M2 and DCs shown for comparison relative to baseline media levels at 5 days. Arginine and serine levels are sufficient to differentiate macrophages and DCs ($p<0.0001$), and M1s and DCs ($p<0.001$).

3.3 Macrophage metabolism altered by culture environments

To analyse the effects on metabolism of culture under various conditions the complete set of identifiable peaks across all samples were studies. Where matched bins related to the same metabolite, these were grouped and a maximum value taken for the metabolite as a whole – reducing the data set and improving the consistency and accuracy of results from noise. Samples of differentiation media, treated identically to the samples, were used as a baseline for graphing purposes.

Additionally, longitudinal analysis was performed with Galgo to rank the identified metabolites for their relative contribution to changes between the studied timepoints. Note as cell media were replaced at each timepoint, relative levels at each timepoint are indicative of production from metabolism over the preceding number of days. Additionally the possibility of ongoing replication cannot be excluded. Therefore, direct comparisons between timepoints are difficult. However, within-timepoint comparisons of differentiated macrophages subsets in various environments are outlined below. In order to account for media replacement, charts of relative change are based on baseline

readings of media, from the same stock and subject to identical treatment as the cultures.

3.3.1.1 Metabolic effects of differentiation under different conditions

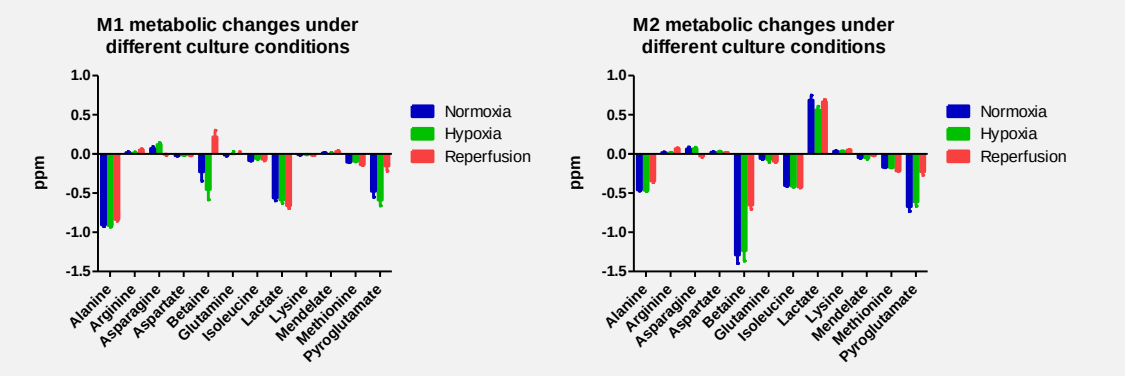

Figure 7. Relative ppm of key metabolites from baseline media to day 5 culture. Note M1 and M2s keep their unique profiles, with minor variations in response to culture conditions.

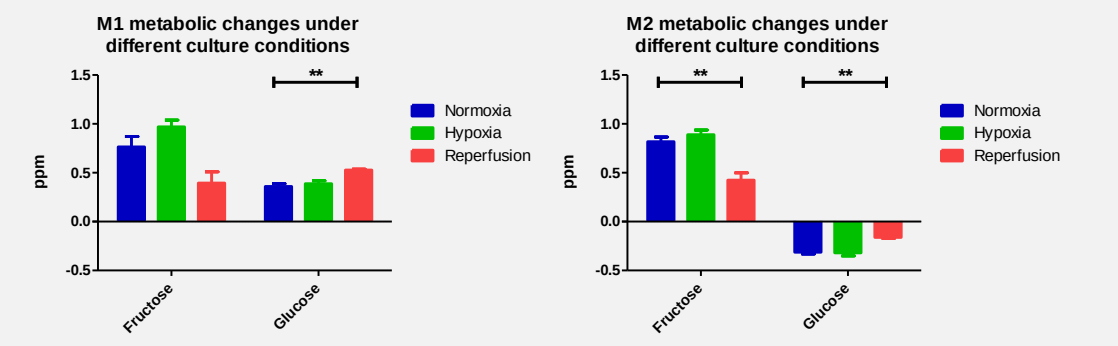

Figure 8. Energy source changes during culture. Note the *increase* in medium glucose in M1 cultures

To assess initial effects of exposure to hypoxic conditions, monocytes were differentiated under various conditions and media were collected at day 5. Metabolic differences arising from both differentiation of the M1 and M2 subsets, and the various culture conditions, are apparent. Base culture media, taken from same time-point, and treated identically to the cultures is used for baseline on these graphs. Therefore, a fall in metabolite levels is indicative of consumption of given metabolite by cells in culture, a rise is indicative of production or release as degradation products.

By day 5 culture under hypoxic conditions, metabolic conditions were broadly unchanged from those outlined previously under normoxia. Most significantly observed is a slight decrease in betaine and pyroglutamate detected in media of hypoxia-cultured M1 macrophages, but not in M2s. Reperfusion culture results in more striking differences, with an *increase* in media betaine in M1 cultures and a reduction in M2s. Also notable in both cultures is a significant *increase* in pyruvate. Perhaps surprisingly, anaerobic culture results in only minor alterations in lactate levels, with both M1 and M2 macrophages maintaining their inverse profiles.

3.3.1.2 Metabolic effects of culture under different conditions

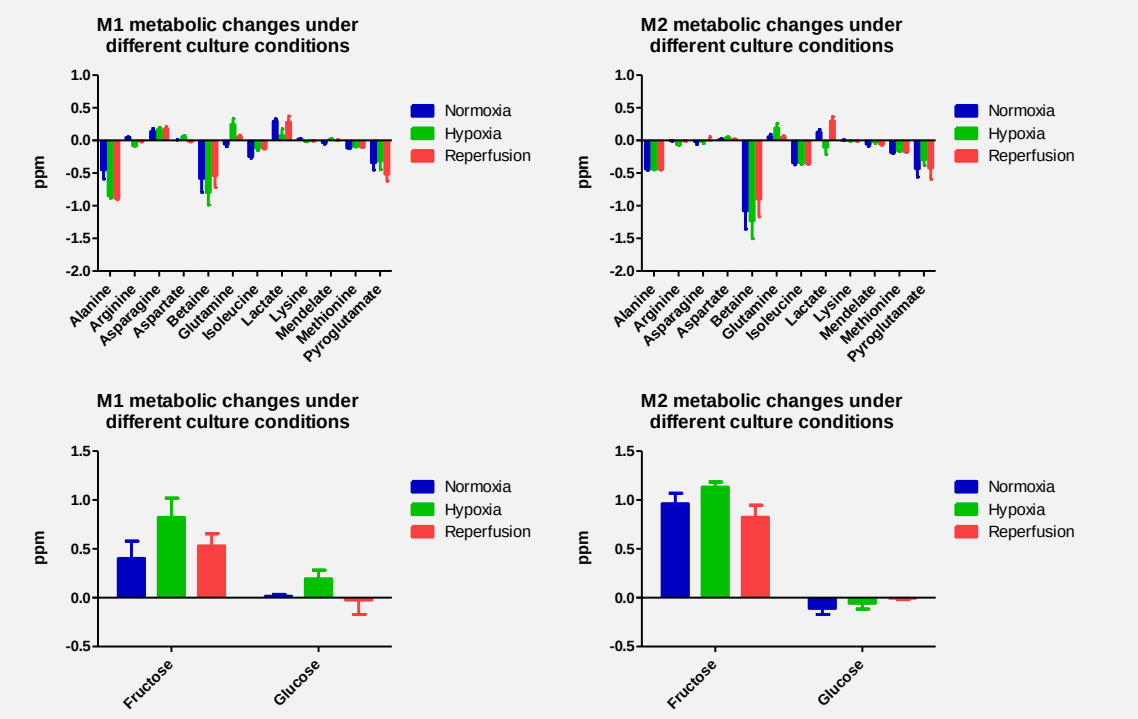

Figure 9. Relative ppm of key metabolites at day 7 of experiment relative to baseline media.

To assess longer term effects of exposure to different oxygenation levels, macrophages were cultured out to 7 days with replacement of differentiation media at regular intervals. Key metabolites identified as differentiating M1 and M2 macrophages, and of culture under different oxygenation levels were considered.

By day 7 of culture a number of subtle changes have occurred. Metabolic profiles of reperfusion-cultured cells tend towards those seen in normoxia particularly with regard to relative levels of betaine and pyroglutamate in media. Both M1 & M2s also display broadly similar profiles for these key metabolites by this timepoint although distinguishing features remain, such as higher levels of alanine in media from M1s under normoxia. Interestingly, the inverse lactate profile seen between M1 and M2s is no longer present, with negative lactate (albeit small) observed in M2s under hypoxia.

3.4 Macrophage metabolism following LPS stimulation

As demonstrated by the IL-10 data oxygenation conditions can have profound effects on the relative responses of M1 and M2 macrophages. To further investigate these effects with regard to the metabolism of these cells, the cell media and extracts of both stimulated and unstimulated cells from the final timepoint were analysed.

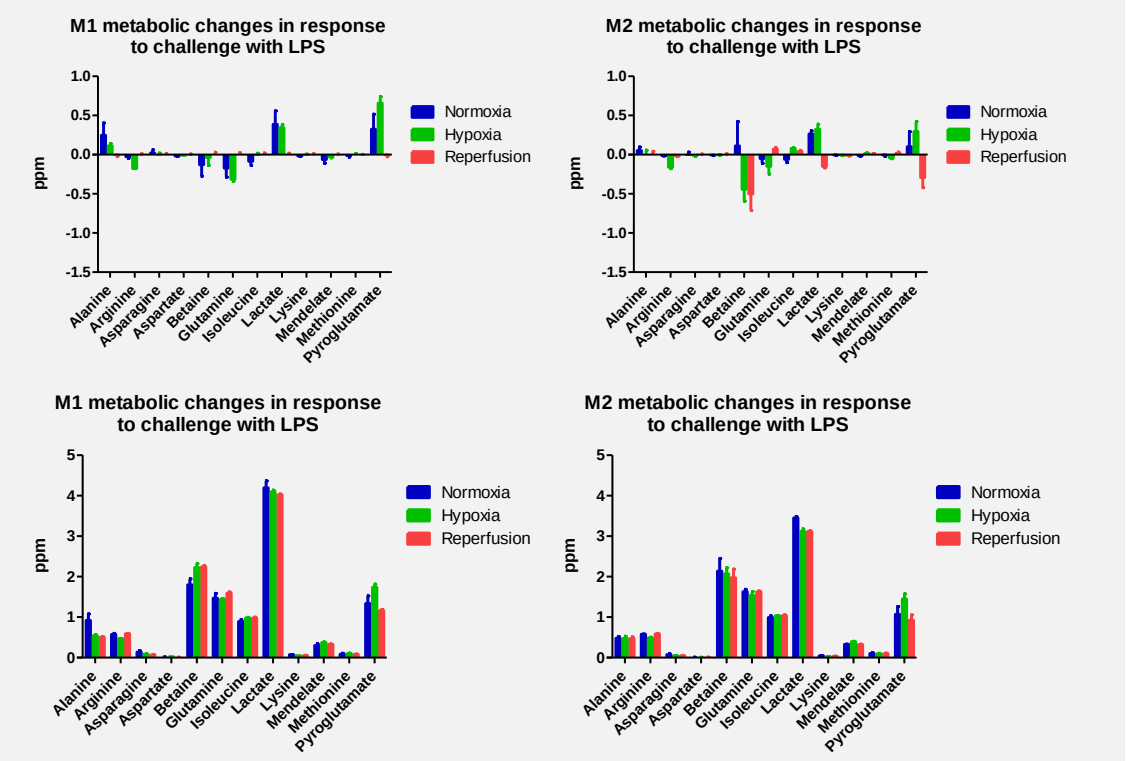

Figure 10. Key metabolites in cell media following LPS stimulation showing relative level of each metabolite from stimulated vs. unstimulated cultures (top) and bare metabolite levels (bottom). Note that although the profiles of M1 and M2s are broadly similar after LPS stimulation, no change is recorded in M1s under reperfusion.

Across the board metabolic responses are relatively muted, however distinct profiles are observed for both M1 and M2s responding to LPS stimulus and under different conditions. Broadly, stimulation with LPS is associated with increases in lactate and pyroglutamate levels in the culture medium under normoxia and hypoxia.

M1 macrophages respond similarly under normoxia and hypoxia, with increases in lactate (as previously observed at early timepoints) and pyroglutamate, and reductions in glutamine and betaine, while under reperfusion culture, little to no metabolic alteration is observed between normal culture and LPS stimulation. In contrast M2s respond to LPS stimulation under reperfusion culture with reductions in betaine, pyroglutamate and lactate levels. Under hypoxic culture both lactate and pyroglutamate are similar to those in stimulated normoxia, although betaine levels are reduced.

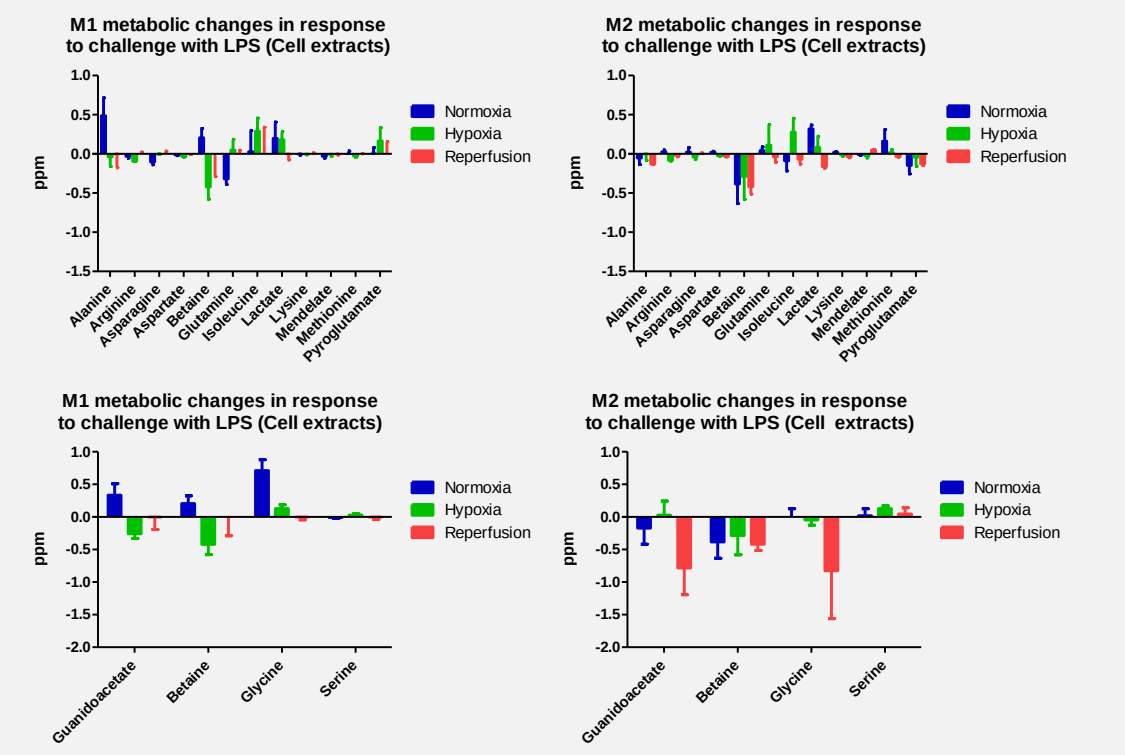

Figure 11. Key metabolites in cell extracts following LPS stimulation showing relative level of from stimulated vs. unstimulated cultures. Relative profiles of both M1 and M2s are similar except for those highlighted in the bottom panel.

Cell extract metabolite levels more variable, perhaps reflecting relative complexity of extraction and preparation process. Interestingly, aside from the key metabolites identified by Galgo in the media, there are considerable differences between M1 and M2 metabolism following LPS stimulation, with M2s recording a significant drop in guanidoacetate, betaine and glycine (a pre-cursor of guanidoacetate).

3.5 IL-10 production confirms differentiation

Production of IL-10 is observed in M1 and M2 macrophages following stimulation with LPS, but not dendritic cells. ELISA assay of culture media following stimulation with LPS confirms the production of IL-10 by both M1 and M2 cultures, but not DC cultures.

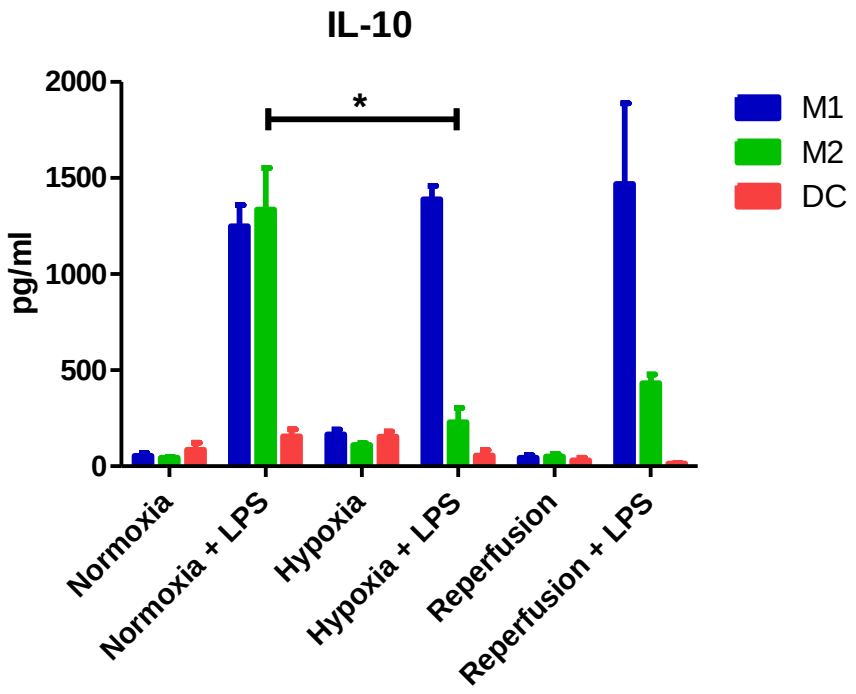

Figure 12. IL-10 production in pg/ml by LPS stimulated differentiated M1, M2 and DCs under normoxia, hypoxia and reperfusion. M2 production of IL-10 is significantly reduced under hypoxic conditions.

3.6 IL-10 production by M2 macrophages is reduced under hypoxia

IL-10 production by differentiated M1, M2 and DCs grown under normoxia, hypoxia and reperfusion was assessed via ELISA. Unstimulated M1, M2 and DCs produce negligible IL-10 under normoxic, hypoxic or reperfusion conditions. A slight increase is observed under hypoxia. Under hypoxia IL-10 production by M1 macrophages remains at comparable levels to that observed under normoxia, while M2 macrophages display significantly reduced levels. Production of IL-10 under reperfusion is between that observed in normoxia & hypoxic conditions.

4 Discussion

Macrophages are a broad family of monocyte-derived cells with a wide range of immunological and non-immunological functions, from clearance of erythrocytes in the liver to release of inflammatory mediators at the site of infection. Specific tissue-resident macrophages are phenotypically adapted to their role, and studies on monocyte culture lineages have shown underlying metabolic differences in these subsets. It is not yet known however the extent to which recruited macrophages, differentiating in the tissues in response to stimulation, differ in their underlying metabolic signatures. As outlined earlier, metabolic differences may have profound effects on the function and effectiveness of these cells, with implications for chronic inflammatory disease.

4.1 Media offers representative indication of cell metabolism

A key requirement for this series of time-course experiments was the ability to perform longitudinal analysis of cellular metabolic function in response to different stimuli. As a result, the availability of a non-destructive method for this analysis was essential and cell culture medium offered a viable solution. However, it was unclear whether the quantity of media the cells were cultured under would dilute relatively minor changes in metabolite quantities, or whether components of the original media would swamp detection. Our first key finding therefore, was that NMR analysis of cell culture media provided comparable and similarly variable levels of detected metabolites, with the notable exceptions of isoleucine and threonine. It is worth noting that the relative levels of metabolites in the media are not solely indicative of culture, but also of metabolites present in the original culture medium. As such the observed similarity may be accounted for by rapid uptake of growth media components by the macrophages in culture. Regardless, the results demonstrate that the conditions in the external media are largely representative of those intracellularly. Subsequent experiments attempted to

correct for the media contribution to metabolite levels by comparison with a baseline analysis of neat media. Unfortunately no such baseline exists for cell extracts, therefore in further study it would be beneficial to perform metabolomics analysis of pre-culture macrophages isolated in the same manner, to ascertain baseline levels of metabolites in primary cells.

4.2 Differentiating monocytes display altered metabolic profiles

In order to determine whether differentiation of monocytes resulted in cells with distinctive metabolic profiles, which in turn may reflect their function, the metabolic profiles of differentiating M1, M2 and DCs were determined at 5 days culture under different conditions. As described the highest ranking metabolite differences, identified by genetic algorithm, include alanine and serine, but with large differences also noted with lactate, pyroglutamate, alanine and isoleucine. It is the profiles of the M1 and M2 macrophages that will be concentrated on here.

Most striking through the early differentiation and culture process is the mirror-image levels of lactate observed in the two macrophage cultures. Observed levels were calculated relative to baseline media samples and show a large reduction in detectable lactate levels in M1 culture, in stark contrast to high levels observed under M2 culture. Lactate is a key component of glycolysis / gluconeogenesis and pyruvate metabolism. Importantly levels of pyruvate detectable in media are unchanged (data not shown) at this time-point, excluding pyruvate metabolism or glycolysis, while levels of glucose are shown to increase. Gluconeogenesis is the metabolic process of formation of glucose from non-carbohydrate sources, and is typically considered restricted to the liver, although one gene variant, PFKFB3 has been shown to be active in a number of human tumour cell lines[37]. Interestingly, the gluconeogenic enzyme fructose-1,6-bisphosphatase has been shown to be activated in monocyte-derived Hl60 line under

vitamin-D3 driven differentiation, and is also found in alveolar macrophages[38]. It is possible that glucose production in M1s is a side effect, as the target of fructose-1,6-bisphosphatase, the glycolysis intermediate fructose-1,6-bisphosphate, also has anti-inflammatory and anti-histiminic functions[39]. M1 macrophages undergoing differentiation may therefore be acting to remove early anti-inflammatory stimulus while providing an energy source to enable rapid expansion of responses in tissues with limited blood supply. This relative excess of glucose in M1 cultures appeared to be short-lived and differentiation-associated. By day 7 levels of glucose in M1 culture had fallen, as had levels of fructose, suggesting either an end of production or demand exceeding synthesis capacity.

The distinct profile of M1 and M2s was largely lost by day 7, with the mirrored levels of lactate returning to comparable levels, with M2s under hypoxia now showing the lowest levels. Metabolic differences therefore appear to be restricted to differentiation and perhaps activation. However, a small but significant drop in arginine levels at day 7 in M1s particularly may coincide with HIF-1 mediated upregulation of genes coding arginases and iNOS[27], which coincide with increased TNFa and IL-6. While nitric oxide has vasodilatory functions, synthesis is paradoxically oxygen dependent. Released as a free radical however, it has potent antimicrobial activity in. In increased hypoxia, a shift towards urea and ornithine production may be expected unfortunately neither metabolite was identifiable from spectra. Interestingly, increased levels of urea have been shown to inhibit the activity of pyruvate kinase, while betaine mitigates this behaviour[40]. Betaine levels were reduced following stimulation in hypoxia.

4.3 Stimulated macrophages have shared metabolic profiles

Stimulation of differentiated macrophages results in a metabolic profile as outlined in Figure 10. It is interesting to note that differences observed between M1 and M2s during

differentiation are no longer apparent, with the exception of slightly higher lactate level in M1s. Relative profiles between stimulated and unstimulated macrophages show a common increase in lactate and pyroglutamate levels in culture and a fall of betaine under hypoxia, and glutamine falling in M1s under normoxia and rising under hypoxia.

4.3.1.1 M1 macrophages, reperfusion and intrinsic activity

The most striking result from the stimulation experiments is the complete absence of metabolic change detectable in stimulated M1 macrophages cultured under reperfusion conditions. It is important to note that results here are relative to unstimulated macrophages cultured under the same experimental conditions. In figure Figure 10 the bare metabolite levels are shown demonstrating that the reperfusion response in M1s is equivalent to those under other conditions. Therefore, rather than indicating a lack of response in reperfusion conditions, the metabolic profile observed may be indicative of instrinsic activation of M1 macrophages under reperfusion conditions.

Because of an association inflammation and hypoxia in the inflamed tissues, the use of hypoxia as a trigger for activation is not suprising. However, while a viable strategy under normal conditions, infiltration of immune cells, including macrophages, to unusual persistently hypoxic sites – such as the rheumatoid synovium – may provide a link from structural hypoxia to abherrant activation. Once initiated, the release of cytokines may drive further infiltration of immune cells to a similar fate, driving a cascade of inflammatory response. Reperfusion injury *in vivo* may be indicative of local tissue damage or a natural effect of monocyte migration from the circulation to injured or damage tissues. Local structural damage in joints provides another route for transient reperfusion via damage to locally inflamed blood vessels.

4.3.1.2 M2 macrophages response to stimulation affected by culture conditions

Stimulation of M2s resulted in the expected increase in lactate and pyroglutamate previously described in both normoxia and hypoxia cultured macrophages. However, under reperfusion a drop in the same metabolites is recorded following stimulation. In contrast betaine levels fall under hypoxia and reperfusion, but increase under normoxia. Levels of fructose are increased relative to un-stimulated macrophages in both hypoxia and reperfusion, while levels of glucose fall - with culture under normoxia showing a mirrored profile suggestive of a switched energy profile in response to low oxygen. However, without further metabolites it is difficult to establish a model of these effects.

4.4 IL-10 responses modulated by hypoxia

A role for IL-10 in modulating inflammatory immune responses can be seen in a number of conditions. In reperfusion injury expression of IL-10 by infiltrating lymphocytes begins at 5 hours post-injury, peaking at 96 hours[41]. In contrast inflammatory responses such as TNFa and IL-6 are initiated almost immediately post-injury. The picture therefore is of a rapid expanding inflammatory response, followed by the gradually suppressive action of IL-10 release either by late arrivals to the inflammatory milieu or changing expression patterns of those already present. It has previously been shown that IL-10 is upregulated[28] in macrophages in response to hypoxic conditions. However, here we have shown that while IL-10 is marginally upregulated in M1 macrophages under hypoxic conditions, production by M2s is strongly inhibited. The resulting balance of IL-10 in any hypoxic inflammatory site therefore is dependent on the relative numbers of M1 and M2 macrophages infiltrating. The discovery that M2s are capable of *in situ* replication in the tissues[14] would suggest an excess would normally persist, therefore, the resolution of any inflammation may be heavily dependent on return to normoxic perfused states. A potential functional benefit of this behaviour *in vivo* is clear, with much reduced inhibition of inflammatory processes in the early stages of infection,

where tissue damage and hypoxia are most severe. As tissue repair processes begin and perfusion returns, suppression of IL-10 release local tissue M2 macrophages is lifted, and the wound site can rapidly resolve. Likewise, the potential for this mechanism to go awry under chronically hypoxic tissues, such as the rheumatoid synovium, is clear.

4.5 Conclusions

Bringing together these findings in an *in vivo* context a picture emerges of M1 macrophages responding pre-adapted for the hypoxic conditions of the inflamed site. Differentiation in the tissues triggers up-regulation of fructose-1,6-bisphosphatase activity, with the dual effect of increasing local glucose – providing abundant energy for local proliferation in poorly perfused tissues – and simultaneous degradation of anti-inflammatory fructose-1,6-bisphosphate. Only by later time-points are typical adaptations to hypoxia initiated, including potentially HIF-1α activation, also seen following LPS stimulation. In contrast, differentiation to M2 is associated with increased lactate production largely independent of oxygen levels in culture. Production of IL-10 following stimulation with LPS is however significantly reduced.

In combination, the effect is of a reduced, or suppressed, anti-inflammatory response during initial infiltration of M1 macrophages, or under hypoxic conditions for M2 macrophages. Together, these may act to prolong inflammation until either migration or M1 differentiation is interrupted, or reperfusion of the hypoxic tissues occurs. In normal, healthy, wounded tissues, this sequence of events may aid to prolong inflammation until resolution is appropriate. However, in chronically inflamed tissues, such as the rheumatoid synovium, persistent hypoxia combined with and aberrant infiltration by M1 macrophages may reinforce, prolong or even drive the pathological process.

Further study would benefit for a wider panel of identified metabolites, together with metabolic pathway mapping to build a fuller picture of these interactions. Due to time constraints all spectra used for this study were 1D, while NMR 2D or 1D JRES spectra separate resonance peaks onto a second axis, excluding or reducing interference from multiple metabolites and greatly simplifying identification, unfortunately at a considerable cost of time. However, single representative 2D spectra may provide sufficient information to build better models.

Finally, key to understanding and interpreting these data is a complete understanding of the underlying processes that govern observations. Metabolic pathways are complex structures and data here described represent an assortment of midpoints and endpoints in these processes. With the addition of microarray gene transcription data it would be possible to characterise the on-going processes in the cell, through observations of changes in metabolic enzymes, and so both map responses and visualise routes from normal activity to chronic pathology.

References

1. Gordon, S. & Taylor, P.R. Monocyte and macrophage heterogeneity. *Nat Rev Immunol* **5**, 953-964 (2005).
2. Mosser, D.M. & Edwards, J.P. Exploring the full spectrum of macrophage activation. *Nat. Rev. Immunol* **8**, 958-969 (2008).
3. Tacke, F. & Randolph, G.J. Migratory fate and differentiation of blood monocyte subsets. *Immunobiology* **211**, 609-618 (2006).
4. Whitelaw, D.M. OBSERVATIONS ON HUMAN MONOCYTE KINETICS AFTER PULSE LABELING. *Cell Prolif* **5**, 311-317 (1972).
5. Sunderkötter, C. et al. Subpopulations of mouse blood monocytes differ in maturation stage and inflammatory response. *J. Immunol* **172**, 4410-4417 (2004).
6. Geissmann, F., Jung, S. & Littman, D.R. Blood monocytes consist of two principal subsets with distinct migratory properties. *Immunity* **19**, 71-82 (2003).
7. Passlick, B., Flieger, D. & Ziegler-Heitbrock, H.W. Identification and characterization of a novel monocyte subpopulation in human peripheral blood. *Blood* **74**, 2527-2534 (1989).
8. Auffray, C. et al. Monitoring of blood vessels and tissues by a population of monocytes with patrolling behavior. *Science* **317**, 666-670 (2007).
9. Chapuis, F. et al. Differentiation of human dendritic cells from monocytesin vitro. *Eur. J. Immunol.* **27**, 431-441 (1997).
10. Gordon, S. Alternative activation of macrophages. *Nat Rev Immunol* **3**, 23-35 (2003).
11. O'Shea, J.J. & Murray, P.J. Cytokine Signaling Modules in Inflammatory Responses. *Immunity* **28**, 477-487 (2008).
12. Kodelja, V. et al. Differences in angiogenic potential of classically vs alternatively activated macrophages. *Immunobiology* **197**, 478-493 (1997).
13. Kreider, T., Anthony, R.M., Urban, J.F. & Gause, W.C. Alternatively activated macrophages in helminth infections. *Current Opinion in Immunology* **19**, 448-453 (2007).
14. Jenkins, S.J. et al. Local Macrophage Proliferation, Rather than Recruitment from the Blood, Is a Signature of TH2 Inflammation. *Science* **332**, 1284-1288 (2011).
15. Erwig, L.-P. & Henson, P.M. Immunological Consequences of Apoptotic Cell Phagocytosis. *The American Journal of Pathology* **171**, 2-8 (2007).
16. Firestein, G.S. Evolving concepts of rheumatoid arthritis. *Nature* **423**, 356-361 (2003).
17. Zhang, X. & Mosser, D. Macrophage activation by endogenous danger signals. *J. Pathol.* **214**, 161-178 (2008).
18. Chen, C.-J. et al. Identification of a key pathway required for the sterile inflammatory response triggered by dying cells. *Nat Med* **13**, 851-856 (2007).
19. Kono, H. & Rock, K.L. How dying cells alert the immune system to danger. *Nat Rev Immunol* **8**, 279-289 (2008).
20. Bental, M. & Deutsch, C. Metabolic changes in activated T cells: an NMR study of human peripheral blood lymphocytes. *Magn Reson Med* **29**, 317-326 (1993).
21. Cham, C.M. & Gajewski, T.F. Glucose availability regulates IFN-gamma production and p70S6 kinase activation in CD8+ effector T cells. *J. Immunol* **174**, 4670-4677 (2005).
22. Murdoch, C., Muthana, M. & Lewis, C.E. Hypoxia regulates macrophage functions in inflammation. *J. Immunol* **175**, 6257-6263 (2005).
23. Young, S.P. et al. Metabolomic analysis of human vitreous humor differentiates ocular inflammatory disease. *Mol. Vis* **15**, 1210-1217 (2009).
24. Young, S.P. & Wallace, G.R. Metabolomic analysis of human disease and its application to the eye. *J Ocul Biol Dis Infor* **2**, 235-242 (2009).
25. Qiao, H. & May, J.M. Macrophage differentiation increases expression of the ascorbate transporter (SVCT2). *Free Radic. Biol. Med* **46**, 1221-1232 (2009).
26. Scannell, G. Leukocyte responses to hypoxic/ischemic conditions. *New Horiz* **4**, 179-183 (1996).
27. Albina, J.E., Henry, W.L., Jr, Mastrofrancesco, B., Martin, B.A. & Reichner, J.S. Macrophage activation by culture in an anoxic environment. *J. Immunol* **155**, 4391-4396 (1995).

28. Murata, Y., Ohteki, T., Koyasu, S. & Hamuro, J. IFN-γ and pro-inflammatory cytokine production by antigen-presenting cells is dictated by intracellular thiol redox status regulated by oxygen tension. *Eur. J. Immunol.* **32**, 2866-2873 (2002).
29. White, J.R. et al. Genetic amplification of the transcriptional response to hypoxia as a novel means of identifying regulators of angiogenesis. *Genomics* **83**, 1-8 (2004).
30. Ertel, W., Singh, G., Morrison, M.H., Ayala, A. & Chaudry, I.H. Chemically induced hypotension increases PGE2 release and depresses macrophage antigen presentation. *Am. J. Physiol* **264**, R655-660 (1993).
31. Lahat, N. et al. Hypoxia reduces CD80 expression on monocytes but enhances their LPS-stimulated TNF-alpha secretion. *J. Leukoc. Biol* **74**, 197-205 (2003).
32. Cramer, T. et al. HIF-1alpha is essential for myeloid cell-mediated inflammation. *Cell* **112**, 645-657 (2003).
33. Lee, J.-W., Bae, S.-H., Jeong, J.-W., Kim, S.-H. & Kim, K.-W. Hypoxia-inducible factor (HIF-1)alpha: its protein stability and biological functions. *Exp. Mol. Med* **36**, 1-12 (2004).
34. Hollander, A.P., Corke, K.P., Freemont, A.J. & Lewis, C.E. Expression of hypoxia-inducible factor 1alpha by macrophages in the rheumatoid synovium: implications for targeting of therapeutic genes to the inflamed joint. *Arthritis Rheum* **44**, 1540-1544 (2001).
35. Blouin, C.C. Hypoxic gene activation by lipopolysaccharide in macrophages: implication of hypoxia-inducible factor 1. *Blood* **103**, 1124-1130 (2003).
36. Brindle, J.T. et al. Rapid and noninvasive diagnosis of the presence and severity of coronary heart disease using 1H-NMR-based metabonomics. *Nat. Med* **8**, 1439-1444 (2002).
37. Chesney, J. An inducible gene product for 6-phosphofructo-2-kinase with an AU-rich instability element: Role in tumor cell glycolysis and the Warburg effect. *Proceedings of the National Academy of Sciences* **96**, 3047-3052 (1999).
38. Solomon, D.H., Raynal, M.C., Tejwani, G.A. & Cayre, Y.E. Activation of the fructose 1,6-bisphosphatase gene by 1,25-dihydroxyvitamin D3 during monocytic differentiation. *Proc. Natl. Acad. Sci. U.S.A* **85**, 6904-6908 (1988).
39. Cuesta, E. et al. Fructose 1,6-bisphosphate prevented endotoxemia, macrophage activation, and liver injury induced by D-galactosamine in rats. *Crit. Care Med* **34**, 807-814 (2006).
40. Burg, M.B., Kwon, E.D. & Peters, E.M. Glycerophosphocholine and betaine counteract the effect of urea on pyruvate kinase. *Kidney Int. Suppl* **57**, S100-104 (1996).
41. Frangogiannis, N.G. et al. IL-10 is induced in the reperfused myocardium and may modulate the reaction to injury. *J. Immunol* **165**, 2798-2808 (2000).